NASA TECHNICAL NOTE

NASA TN D-8179

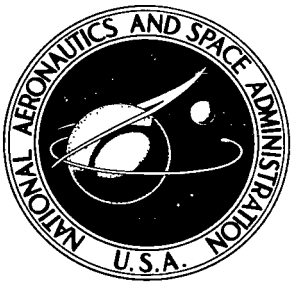

NASA TN D-8179

IMPACT DYNAMICS RESEARCH FACILITY FOR FULL-SCALE AIRCRAFT CRASH TESTING

Victor L. Vaughan, Jr., and Emilio Alfaro-Bou

Langley Research Center
Hampton, Va. 23665

NATIONAL AERONAUTICS AND SPACE ADMINISTRATION • WASHINGTON, D. C. • APRIL 1976

1. Report No.	2. Government Accession No.	3. Recipient's Catalog No.
NASA TN D-8179		

4. Title and Subtitle
IMPACT DYNAMICS RESEARCH FACILITY FOR FULL-SCALE AIRCRAFT CRASH TESTING

5. Report Date
April 1976

6. Performing Organization Code

7. Author(s)
Victor L. Vaughan, Jr., and Emilio Alfaro-Bou

8. Performing Organization Report No.
L-10514

9. Performing Organization Name and Address
NASA Langley Research Center
Hampton, Va. 23665

10. Work Unit No.
505-02-13-01

11. Contract or Grant No.

12. Sponsoring Agency Name and Address
National Aeronautics and Space Administration
Washington, D.C. 20546

13. Type of Report and Period Covered
Technical Note

14. Sponsoring Agency Code

15. Supplementary Notes

16. Abstract

An impact dynamics research facility (IDRF) has been developed to crash test full-scale general aviation aircraft under free-flight test conditions. The aircraft are crashed into the impact surface as free bodies; a pendulum swing method is used to obtain desired flight paths and velocities. Flight paths up to -60° and aircraft velocities along the flight paths up to about 27.0 m/s can be obtained with a combination of swing-cable lengths and release heights made available by a large gantry.

Seven twin engine, 2721-kg aircraft have been successfully crash tested at the facility, and all systems functioned properly. Acquisition of data from signals generated by accelerometers on board the aircraft and from external and onboard camera coverage has been successful in spite of the amount of damage which occurred during each crash.

Test parameters at the IDRF are controllable with flight-path angles accurate within 8 percent, aircraft velocity accurate within 6 percent, pitch angles accurate to 4.25°, and roll and yaw angles acceptable under wind velocities up to 4.5 m/s.

17. Key Words (Suggested by Author(s))
Crashworthy
Crash simulation testing
General aviation aircraft

18. Distribution Statement
Unclassified – Unlimited

Subject Category 03

19. Security Classif. (of this report)	20. Security Classif. (of this page)	21. No. of Pages	22. Price*
Unclassified	Unclassified	56	$4.25

*For sale by the National Technical Information Service, Springfield, Virginia 22161

CONTENTS

IMPACT DYNAMICS RESEARCH FACILITY FOR FULL-SCALE AIRCRAFT CRASH TESTING

Victor L. Vaughan, Jr., and Emilio Alfaro-Bou
Langley Research Center

SUMMARY

An impact dynamics research facility (IDRF) has been developed to crash test full-scale general aviation aircraft under free-flight test conditions. The aircraft are crashed into the impact surface as free bodies; a pendulum swing method is used to obtain desired flight paths and velocities. Flight paths up to -60° and aircraft velocities along the flight paths up to about 27.0 m/s can be obtained with a combination of swing-cable lengths and release heights made available by a large gantry.

Seven twin engine, 2721-kg aircraft have been successfully crash tested at the facility, and all systems functioned properly. Acquisition of data from signals generated by accelerometers on board the aircraft and from external and onboard camera coverage has been successful in spite of the amount of damage which occurred during each crash.

Test parameters at the IDRF are controllable with flight-path angles accurate within 8 percent, aircraft velocity accurate within 6 percent, pitch angles accurate to 4.25°, and roll and yaw angles acceptable under wind velocities up to 4.5 m/s.

INTRODUCTION

The Langley Research Center has recently converted the lunar landing research facility into an impact dynamics research facility (IDRF) for investigating structural crash effects on general aviation type aircraft. A unique feature of this facility is the ability to crash test full-scale aircraft under free-flight conditions and, at the same time, to control the impact attitude and velocity of the aircraft. Full-scale aircraft crash simulation tests have been conducted to obtain definitive data on the structural response of aircraft and on the loads transmitted to the occupants during a crash impact. These data can be used for correlation with results of analytical predictive methods. Full-scale aircraft crash tests can also be used to evaluate crashworthy design concepts both for the aircraft structure and for seat and restraint systems.

This report describes the IDRF, its operation, and the measure of performance of the facility and associated systems.

SYMBOLS

t	free-flight time, seconds
t_u	umbilical separation time (elapsed time between swing-cable separation and umbilical separation), seconds
V	velocity of aircraft along flight path at impact, meters/second
V_h	horizontal velocity of aircraft at impact, meters/second
V_v	vertical velocity (sink speed) of aircraft at impact, meters/second
X,Y,Z	coordinate axes
α	angle of attack of aircraft at impact, degrees
γ	flight-path angle of aircraft at impact, degrees
θ	pitch angle of aircraft at impact, degrees
θ_e	pitch angle error of aircraft due to catenary effects, degrees
ϕ	roll angle of aircraft at impact, degrees
Ψ	yaw angle of aircraft at impact, degrees

FULL-SCALE AIRCRAFT CRASH-TEST TECHNIQUE

The test technique used to crash full-scale aircraft is shown schematically in figure 1. The aircraft, suspended by two swing cables, is drawn back above the impact surface to a predetermined height by a pullback cable. The test sequence is initiated when the aircraft is released from the pullback cable. The aircraft swings pendulum style into the impact surface. The swing cables are pyrotechnically separated from the aircraft a short distance above the impact surface, freeing the aircraft from restraint during the crash impact. The umbilical (fig. 1) remains attached during the impact for data acquisition and is pyrotechnically separated at a predetermined time after swing-cable separation.

In figure 2, the flight-path and attitude angles of the aircraft at impact are identified together with the axes and force directions. The flight-path angle, which can be adjusted

up to -60° (see fig. 1), is determined by the length of the swing cables. The height (49 m maximum) at which the aircraft is suspended above the impact surface determines the impact velocity along the flight path; that velocity can be varied up to 27 m/s.

In the suspended position, it is important that the force vectors of the swing cables and pullback cable act at an angle of 90° to each other and pass through the center of gravity (c.g.) of the aircraft. This relation must be established, as close as the swing-cable catenary allows, in order to achieve maximum control of aircraft pitching during the swing phase of the test. The pitching velocity of the aircraft at swing-cable separation continues to change the pitch attitude of the aircraft during the free-flight phase of the test. The swing-cable catenary introduces pitch error into the system.

For any planned set of aircraft crash-test parameters, the test geometry of the facility necessary to obtain the parameters can be calculated using the equations presented in appendix A. The equations do not consider the effects of local pitching-inertial forces after swing-cable separation nor do they consider catenary effects.

FACILITY AND ASSOCIATED SYSTEMS

Gantry Structure

The basic structure used in the development of the IDRF is the gantry of the former lunar landing research facility. The gantry (fig. 3) is oriented in the east-west direction and is composed of truss elements arranged with three sets of inclined legs to give vertical and lateral support; one set of inclined legs at the east end provides for longitudinal support. The gantry is 73 m high and 122 m long. The supporting legs are spread 81 m apart at the ground and 20 m apart at the 66-m level. An enclosed elevator and a stairway provide access to the overhead work platforms. Catwalks permit safe traverse of the gantry. A movable bridge spans the gantry at the 66-m level and traverses the length of the gantry.

Major Features

Figure 4 presents an isometric drawing of the IDRF. Two pivot-point platforms, located at the west end of the gantry, support the 26.7-kN capacity winches and sheave systems for controlling the length of the swing cables. The sheave system contains cable locks which serve to protect the winches from overload and dynamic reactions.

A pullback platform located on the underside of the movable bridge supports another 26.7-kN capacity winch and sheave system for controlling the length of the pullback cable. The movable bridge can be positioned so that the angle between the pullback and swing cables can be set to the desired 90°. The platforms and cable systems have been operated

with aircraft of a nominal gross mass of 2721 kg and a dynamic swing load of 2g. However, with modified cable arrangements (block and tackle type) for reducing the forces on the winches, the systems can be used to crash test aircraft up to 14 000 kg gross mass.

The gantry structure contains two umbilical platforms (fig. 4), one on the west bent and one on the center bent of the gantry. Each platform contains an umbilical storage box, an umbilical winch for controlling the length of the umbilical cable, camera mounts, and an instrumentation junction box. The junction box is hard wired to another junction box in the control room.

The impact surface is a 121-m-long, 9.0-m-wide, strip of reinforced concrete with 0.2-m thickness. A 1.0-m-square grid is painted on the concrete surface for use as a photographic background for cameras mounted at the top of the gantry. Adjacent to the impact surface is a 30-m-long by 12-m-high photographic backboard with a 1.0-m-square grid for ground camera reference. The backboard is mounted on rails to accommodate a crash test at any position along the impact surface.

Aircraft Suspension System

The swing cables and pullback cable connect to the aircraft swing and pullback harnesses which make up the aircraft suspension system as illustrated in figure 5. The harnesses are designed specifically for the aircraft configuration being tested.

The swing harness consists of two swing-cable extensions and two sets of pitch cables. The swing-cable extensions attach to hard points mounted to the main spar of the aircraft wing. The pitch cables are attached to the swing-cable rings located at the upper end of the swing-cable extensions and to hard points in the fuselage fore and aft of the aircraft center of gravity.

The pullback harness consists of two cables which connect to the pullback cable and to the hard points mounted to the main spar of the aircraft wing. A spreader bar separates the two harness cables aft of the fuselage. Thus, the aircraft stabilizers can pass between the cables, and the bar clears the fin as the pullback cable rises above the empennage during the lift of the aircraft.

The swing-cable extensions and pullback harness cables attach to the same hard points. These hard points are located so that a line drawn between them passes directly through the center of gravity of the aircraft. Therefore, the force vectors of both the swing and pullback cables pass through the center of gravity of the aircraft and the aircraft is free to pitch around its own center of gravity. The two sets of pitch cables restrain the aircraft in the planned angle of attack during the preparation and swing phases of the test sequence. When the aircraft is in the pullback release position, the forward pitch cable must also support a load imposed by a moment around the aircraft center of

gravity as a result of the umbilical attachment. A 0.76-cm steel support cable is sandwiched into the umbilical wires to carry loads and to protect the data wires from damage caused by unintentional induced tensile loads. This cable passes through the top of the fuselage and the end attaches to the main spar of the wing near the aircraft center of gravity. The data wires are connected to receptacles mounted on top of the fuselage 1.1 m above the center of gravity of the aircraft. The mass of the umbilical acting at this connection creates a pitching moment around the aircraft center of gravity. This umbilical cable load and accompanying moment varies with drag on the umbilical and is not compensated for during the swing phase of the crash test.

The aircraft attitude is adjusted by changing the length of the cables in the suspension system. Adjustments up to about 30^{o} can be made in angle of attack and roll angle. Only small adjustments can be made in yaw angle because of the small clearance between the pullback harness and empennage of the aircraft. Additional yaw can be added by removing the stabilizers and simulating them with concentrated masses.

Aircraft Release and Separation Systems

The pullback release system and the swing and umbilical separation systems are shown in figure 6. The sequence of pyrotechnic events during the test are: (1) the aircraft is pyrotechnically released from the pullback harness and the aircraft begins to swing; (2) the swing harness pyrotechnically separates from the aircraft at a predetermined height above the impact surface; and (3) the umbilical cable pyrotechnically separates from the aircraft during skid after impact.

The ends of the pullback harness cables attach to the hard points on the wings of the aircraft with low-shock pyrotechnic nuts. (See fig. 6(b).) The attachments are self-alining to eliminate side loads on the nuts. Power to fire the pyrotechnic nuts is transmitted from a power supply in the control room; the power runs through a key-lock switch to the top of the gantry and down a flexible power cable suspended from the gantry, terminating at the pyrotechnic nuts.

The swing and umbilical separation systems are independent of the pullback release system. The ends of the swing-cable extensions attach to hard points on the wing of the aircraft with low-shock pyrotechnic nuts, in a manner similar to those used for attaching the pullback harness cables. (See fig. 6(b).) The pitch cables contain guillotine-type pyrotechnic cable cutters at the surface of the fuselage. (See fig. 6(c).) The umbilical wires terminate in several 55-pin connectors mounted at the top of the fuselage in pyrotechnic-mechanical disconnect assemblies (fig. 6(d)). The steel support cable that carries the tensile loads imposed on the umbilical contains a nylon separation link and guillotine-type pyrotechnic cable cutter.

The swing-cable harness and umbilical pyrotechnic units are fired by a capacitance discharge circuit with the use of a shock-mounted, integral, onboard programer and power supply. The programer contains a safe-arm unit which is activated through the umbilical from a key-lock switch in the control room. The swing-cable harness pyrotechnic units are fired when a lanyard system (see fig. 6(a)) activates the firing circuit at a predetermined distance above the impact surface. The system consists of a switch mounted on the aircraft; the switch is closed by pulling a pin. A 0.17-cm-diameter steel cable is attached and safety wired to the pin. The cable extends through a sheave system attached to the top of the gantry, down through a sheave attached to a light mass (which rides the cable and furnishes a small amount of tension in the cable), and back to the top of the gantry where the end of the cable is anchored. (See fig. 6(a).) A stop attached to the cable on the backside of the lanyard sheave is adjusted to contact the sheave mounting fixture; the pin is pulled as the aircraft swings along the arc path, thus pyrotechnically separating the swing-cable system from the aircraft. A preset timer in the onboard programer is started when the pin is pulled and thus fires the umbilical pyrotechnic disconnects and support cable cutter about 0.75 s after swing-cable separation.

Control Room

Operation of the facility is directed from the control room. (See fig. 4.) Figure 7 is a photograph of the operations panel in the control room. The room is equipped with controls for arming the onboard pyrotechnic programer, turning on interior photographic lights on board the aircraft, releasing the aircraft from the pullback cable, and activating the automatic circuit to the cameras. Two-way communications are provided throughout the facility: intercommunications (head set and mike), public address, and portable radio systems which are all under the supervision of the control room personnel. The facility weather station provides wind velocity and direction readout from the wind vane at the 46-m level of the gantry. The countdown station consists of a countdown clock and the countdown boards. The boards display the sequence of events for the crash test. The entire crash area and gantry structure can be observed from the control room and security is maintained by fences and guards.

DATA-ACQUISITION SYSTEMS

Primary data acquisition during a full-scale aircraft crash test consists of recording signals generated by instruments on board the aircraft and photographing the aircraft during the test.

Instrumentation and Recording System

The onboard instrumentation may consist of accelerometers (both piezoelectric and strain-gage type), strain gages, load cells, and extensometers. The primary data-signal generating instruments are the accelerometers. Figure 8(a) presents a typical accelerometer layout for an aircraft. The circles in the plan view of the aircraft and the vertical diamonds in the elevation view of the aircraft measure accelerations normal to the aircraft horizontal plane. The diamonds oriented parallel to the aircraft longitudinal axis measure accelerations in the longitudinal direction and the filled diamonds measure accelerations in the lateral direction. Figure 8(b) presents a typical triaxial accelerometer installation.

Data signals from the aircraft instrumentation are transmitted by the umbilical cable to the 100-channel junction box on the appropriate umbilical platform at the top of the gantry. (See figs. 1 and 4.) Hard wire connects the junction box to a similar junction box in the control room, and thus gives the facility a data transmission capability of 100 channels. The data-acquisition equipment in the control room is identified in figure 9. The equipment consists of five FM tape recorders, each capable of recording 14 channels of data, and associated data-conditioning equipment. One channel on each recorder is used to record the time code from an IRIG-A time code generator. The data on each recorder can be identified and correlated with respect to time increment. One channel is used to record the signal from a Doppler radar unit used to measure the horizontal velocity of the aircraft at surface contact (impact).

Photographic Coverage

Photographic coverage of the exterior of the aircraft during a crash test is provided by cameras on the ground and at the top of the gantry. (See fig. 4.) Each of the two umbilical platforms located on the gantry contains mounts for two cameras which view the center of the crash area from overhead. A movable camera platform capable of handling three cameras is located on the south side of the gantry structure and can be positioned along the gantry so that the cameras can film the crash area from overhead at a slightly skewed angle to the impact surface. One of the cameras located on the movable platform is used to measure the yaw angle of the aircraft at impact and can be used to determine the approximate horizontal velocity of the aircraft. There is camera coverage from the ground on each side and in front of the crash area. There are provisions for four fixed cameras and four scanning cameras on a portable platform at ground level; this platform can be positioned to permit filming of the crash area at right angles to the impact surface center line. The scanning cameras scan the entire test from pullback cable release until the aircraft comes to a full stop. One of the fixed cameras is used to determine the pitch angle of the aircraft at impact, the flight-path angle, and the

velocity along the flight path. There are provisions for two additional cameras at ground level along the impact surface center line at a distance of about 61 m from the west end of the gantry structure. These cameras look directly into the front of the aircraft and are used to determine the roll angle of the aircraft. There is a single camera located behind the photographic backboard with its lens protruding through a hole in the board. This camera films the crash area at right angles to the impact surface center line.

With the exception of the scanning cameras, all cameras are activated from the control room by an energizing circuit which is controlled from the pullback cable release circuit. The scanning cameras are the only ones which are operated manually and are manned during a test. All cameras receive either IRIG-A time code or standard 60-cycle timing which is used to correlate the film data with the recorded data. Three 70-mm motion-picture cameras and two TV cameras are available. All other cameras use 16-mm film. Film speeds of 8 to 8000 pictures per second (pps) are available, but the most common speeds used are 20, 24, 400, and 2000 pps.

Photographic coverage of the interior of the aircraft during a crash test is provided by cameras mounted in the front, rear, and at the starboard side of the fuselage. (See fig. 10(a).) Figure 10(b) is a photograph of the front camera mounted in the instrument panel, looking aft with primary emphasis on the pilot and copilot. A fisheye lens is used on this camera because of the close proximity of the pilot and copilot to the camera. Figure 10(c) is a photograph of the camera mounted in the aft portion of the aircraft fuselage, looking forward with a full view of the interior of the aircraft cabin. Figure 10(d) shows the two side-mounted cameras. The top camera records the reactions of the first passenger on the port side of the fuselage to the simulated crash. The lower camera records the reaction of the base of the seat to the simulated crash. All cameras on board use 16-mm film running at film speeds of 400 pps. An onboard timing-light signal generator activates a light in each camera, marking the film at time intervals of 0.01 s.

AIRCRAFT CRASH-TEST SPECIMEN

Typical aircraft specimens which have been crash tested are shown in figure 11. The stripped aircraft specimen (fig. 11(a)) consists of a fuselage structural shell, wings with nacelle fairings, and landing gear. The mass and center of gravity of the empennage are simulated by two concentrated masses representing the fin-rudder and stabilizer-elevator combinations. The ailerons and flaps are simulated by concentrated masses. The masses and centers of gravity of the engines are represented either by old engines loaded with lead or by simulated engines made of steel plate and loaded with lead. Concentrated masses are also used to simulate the propellers and spinners.

The complete aircraft (fig. 11(b)) has all the major aircraft parts and equipment necessary to a flightworthy aircraft except the propellers and spinners which are simulated as with the stripped aircraft.

Interior views of the stripped and complete aircraft are shown in figures 11(c) and 11(d). Since the basic aircraft configuration is the same, the interiors of each must be arranged and equipped so that the total weight, balance, and center-of-gravity locations are the same. Only slight variations can be tolerated if control of the test parameters is to be maintained. Various arrangements of seats, anthropomorphic dummies, and restraint systems can be selected for testing as shown by a comparison of figures 11(c) and 11(d). The stripped aircraft does not have floor boards, instrument panel, or furnishings (except seats). Both test specimens contain batteries, instrumentation junction boxes, pyrotechnic programer, and various electrical junction boxes and circuits as needed to prepare the aircraft for crash testing. Additional mass in concentrated form is used in the stripped aircraft to simulate some of those items which are integral to the complete aircraft. Aircraft crash-test preparations common to both the stripped and complete aircraft are given in appendix B.

TEST OPERATIONS

The test operations are carried out in three phases. In the first phase, the aircraft is prepared according to appendix B. The second phase lasts approximately 1 week; this phase consists of moving the aircraft into position under the gantry, integrating the aircraft with the facility, and making the final preparation of the aircraft for testing. The third phase of the test operations is the actual aircraft crash test. All the operations are directed from the control room with the use of countdown procedures which identify all the necessary steps for conducting a safe test. A discussion of the primary test operation activities in condensed form is presented in the following sections.

Aircraft-Facility Integration

There are four primary position alinements (see fig. 12) which must be made to satisfy the test parameters. The alinement dimensions which identify these positions are determined by the measurements and equations of appendix A. The aircraft is alined in position with the use of transits for sighting targets on the aircraft from survey monuments. These monuments are located on the gantry center line and 30 m to the side of the center line. The side monuments are located at distances K, K_{CS}, and P from the pivot-point monument. The movable bridge is also alined in position from a side monument at a distance S from the pivot-point monument.

The impact attitude-alinement position is located directly under the pivot points. (See fig. 12(a).) The aircraft is lifted above the impact surface with the swing cables; only the extension cables of the swing harness are used. The aircraft is adjusted for zero roll and is balanced until the aircraft maintains zero pitch without restraints. The aircraft is lowered to the impact surface and the preadjusted pitch cables are installed. The aircraft is then lifted above the impact surface; the roll angle and angle of attack are set according to the parameters and the yaw angle is set to zero. These angles are set by adjusting the length of the swing-harness cable turnbuckles. The alinement is determined by an inclinometer and transits. This alinement fixes the impact attitude of the aircraft with respect to the swing cables as illustrated in figure 12(b).

The pullback harness and umbilical cable are attached to the aircraft and the aircraft is pulled back near the impact position. (See fig. 12(a).) The length of the swing cables and pullback cable are adjusted until the aircraft is as close to the impact surface as possible, and the target on the aircraft is the distance K from the pivot points. (See fig. 12(c).) If a yaw angle other than zero is required, the final aircraft attitude alinement is made in the impact position. The umbilical cable length is adjusted and marked for reference. The swing cables are now fixed at their correct lengths and marked at the pivot-point platforms for reference. The attitude and location of the aircraft in the impact position are those which should occur at touchdown during the crash test.

The aircraft is then pulled back until the aircraft target is at the distance K_{cs} from the pivot points; this step places the aircraft in the cable-separation position. (See fig. 12(d).) The slack is taken out of the lanyard system cable, and the cable is marked for installation of the lanyard stop. (See fig. 6(a).)

The aircraft is pulled back into the pullback release position as set by dimension P from the pivot points and the height R from the impact surface. (See fig. 12(e).) Using a transit, the height is set by triangulation with a preset angle determined by the calculated height of the aircraft target above the horizontal position of the transit and the measured distance from the transit to the gantry center line. A final check is made of the aircraft alinement and all auxiliary lines are marked so that the positions can be reestablished with minimum effort.

The aircraft is returned to the impact surface for the final preparation which includes instrument installation and check-out, a final check of electrical circuits, battery charging, the installation and check-out of all cameras and circuits, a final check-out of the pyrotechnic circuits, and the installation of pyrotechnic units.

Aircraft Crash-Test Operations

With all preparations complete, the aircraft is recycled through the four positions previously described. The adjusted attitude of the aircraft is rechecked for compliance.

The aircraft is pulled back past the impact position, the swing cables are set to the alinement marks, and the aircraft is lowered with the pullback cable to the impact position. Photographs are taken for reference. The aircraft is pulled back past the cable-separation position and the lanyard stop is installed at the mark on the cable. The aircraft is pulled back to the pullback release position and all lines are set at the reference marks. The gantry and test area are cleared of personnel and all test stations are checked for readiness. The following actions are then taken in the control room:

(1) Instrumentation zeros are recorded.

(2) The pyrotechnic system is armed.

(3) Power supplies are turned on.

(4) Aircraft release switch is unlocked.

(5) Tape recorders are turned on.

(6) Onboard photographic lights are turned on.

(7) The aircraft is released.

The crash test starts when the aircraft is released and starts to swing. When the aircraft reaches the cable-separation position, the lanyard system activates the pyrotechnic circuit and the cables separate from the aircraft. The aircraft, under free-flight conditions, contacts the surface at the impact position. The umbilical separates from the aircraft during the skid before the aircraft comes to a stop. The test is complete when all systems have been secured.

FACILITY AND SYSTEM PERFORMANCE

Typical Aircraft Crash Test

There have been seven full-scale aircraft crash tests performed at the IDRF from January 1974 to July 1975. Figure 13 shows a sequence of photographs taken at 0.05-s intervals during an aircraft crash test (number 6) considered to be typical. The aircraft crashed at a velocity of 26.88 m/s along a -16.5° flight path and at a pitch angle (defined as the impact angle) of 14°. The photograph (fig. 13(a)) shows that the aircraft is in free flight at the time of impact since the swing cables have separated from the aircraft. Most of the vertical velocity of 7.63 m/s is dissipated 0.15 s after impact but very little of the longitudinal velocity has been dissipated. During this period, the aircraft has gone through two impacts: the primary impact when the aft fuselage contacts the impact surface (see fig. 13(a)) and the secondary impact when the aircraft slams down onto the surface because of fuselage rotation. (See fig. 13(d).) The secondary impact can usually be distinguished, in a photographic sequence, as the first photograph showing the aircraft

wings flat on the impact surface (fig. 13(d)). There is little rebound after secondary impact, and most of the remaining energy is dissipated by friction during the aircraft skid.

Typical Crash-Test Data

Figure 14 shows typical acceleration time-history traces obtained during an aircraft crash test (number 6). Figure 14(a) shows a recorded signal (raw data) in digitized form from an accelerometer oriented normal to and mounted on the floor beam at the door of the aircraft shown in figure 13. Figure 14(a) also shows the processed acceleration trace, an average derived from the digitized data using a least-squares fit, superimposed on the raw data trace. Figure 14(b) is a display of the least-squares fit trace to an expanded acceleration scale.

The least-squares fit represents an average of the raw digitized data and exhibits no time lag with respect to the raw data; thus the least-squares fit is suitable for time correlation with data from high-speed cameras.

The traces in figure 14 represent the acceleration time history of the aircraft structure which first contacted the impact surface. (See fig. 13(a).) A sudden acceleration of about -660g (negative sign represents upward direction) is felt by the structure at the point of impact. The time duration of the sharp pulse was approximately 2 ms. The least-squares fit trace shows an acceleration peak of -275g with a time duration of 5 ms, and the trace continues to oscillate until the oscillation damps out at approximately 0.11 s.

Figure 15 shows three typical photographic prints made from single frames of the 16-mm film taken on board the aircraft early in the crash test of figure 13. The cabin of the aircraft is small and all movies taken on board show some distortion because of the lens size necessary to view the areas of interest at such close range. The onboard scenes are typical of the high-speed motion pictures (400 pps) obtained during all seven aircraft crash tests.

Facility Performance Results

The planned crash-test attitude and velocity for each test are: flight-path angle, angle of attack, pitch angle, roll angle, yaw angle, and aircraft velocity along the flight path. The angles are defined in figure 2.

The measure of performance of the IDRF is the accuracy with which the planned parameters are met during the actual crash test. A comparison between the planned parameters and the actual test parameters obtained during the seven aircraft crash tests is presented in table I. The free-flight time is that period between swing-cable separation and the first contact of the aircraft with the impact surface. The flight path is measured as the track of the center of gravity of the aircraft during the free-flight phase of

the test. The pitching velocity is determined from the change in pitch angle during the free-flight time. The umbilical release time is the period between swing-cable separation and umbilical separation. For tests in which the aircraft landing gears are extended, impact is defined as the time at which the landing gear first contacts the impact surface. When landing gears are retracted, impact is defined as the time at which the fuselage makes initial contact with the impact surface. (See fig. 16.)

The first aircraft was crash tested at a velocity of 12.66 m/s along a flight path of -16.75° and a pitch angle of -15.75°. This test was used primarily as a check of the facility systems and test procedures and was the only test performed at this low velocity. The wind velocity was variable up to 4.5 m/s from the west. All test parameters obtained were close to those planned. All systems except the umbilical separation functioned properly. The umbilical failed to separate because the pyrotechnic battery discharged when the pyrotechnic circuit was shorted by part of the damaged aircraft structure. Care was taken on subsequent tests to place circuit wirings in safer locations.

Aircraft tests 1, 2, 4, 6, and 7 were performed with the landing gears retracted. Tests 3 and 5 were performed with the landing gears extended. A comparison of planned and actual test parameters, as given in table I, indicate the following: For all seven tests the flight-path angles were accurate to within 8 percent, flight-path velocities were accurate to within 6 percent, and the angles of attack over the range of values from zero to 30° were accurate to within 4.0°.

The pitch angles, which are dependent on the flight-path angles and angles of attack, were accurate to within 4.25°. The accuracy of the pitch angle reflects inaccuracies in flight-path angles and angles of attack. The error in pitch angle is composed of two primary ingredients: an error introduced by the catenary effects in the swing cables (3.0° or less) and a deviation from the calculated angular rotations of the aircraft in free flight after cable separation (1.0° or less). This error also reflects the effect of flight-path inaccuracies caused by cable-separation position. The analysis of the performance characteristics of the facility is presented in detail in appendix A.

All aircraft crash tests performed at the facility are weather dependent. Wind velocities must be less than 4.5 m/s to insure adequate control of yaw and roll of the aircraft. Winds of greater velocity can cause conditions which can result in larger errors in the aircraft attitude at impact. During test 5 a southeast wind at a velocity of about 8.5 m/s was experienced. The wind caused roll and yaw angle errors of approximately 3.5° and displaced the aircraft 1.0 m laterally from the impact target. All other tests were made with wind velocities of less than 4.5 m/s and the aircraft experienced negligible roll and yaw errors, as can be seen in table I.

CONCLUDING REMARKS

A facility has been developed to crash test full-scale light aircraft under free-flight test conditions at flight paths up to -60° and at velocities along the flight path up to about 27.0 m/s. There have been seven successful aircraft crash tests performed at the facility and all systems functioned properly. Data acquisition of signals from instrumentation on board the aircraft has been collected with minimal loss of data. Film coverage both of the structural behavior and of the detailed collapse of the aircraft during impact has been good from both onboard and external cameras.

The performance of the impact dynamics research facility is highly satisfactory over the range of test parameters selected. The range included: flight-path velocities from 13 to 27 m/s; flight-path angles from -15° to -45°; angles of attack from 0° to 30°; and pitch angles from 15° to -45°. The planned parameters were within the following tolerances:

(1) The flight-path velocity of the aircraft at impact is accurate within 6 percent.

(2) Flight-path angles are accurate within 8 percent.

(3) Pitch angle is accurate within 4.25°.

(4) The roll and yaw angles are acceptable for wind velocities up to 4.5 m/s.

Langley Research Center
National Aeronautics and Space Administration
Hampton, Va. 23665
February 11, 1976

TABLE I.- COMPARISON OF ACTUAL AND PLANNED AIRCRAFT CRASH-TEST PARAMETERS

Parameter	NASA test 1		NASA test 2		NASA test 3		NASA test 4		NASA test 5		NASA test 6		NASA test 7	
	Planned	Actual	Planned	Actual	Planned	Actual	Planned	Actual	Planned	Actual	Planned	Actual	Planned	Actual
Flight-path angle, γ, deg	-16.75	-16.75	-16.75	-16.00	-18.97	-18.75	-15.96	-14.75	-18.97	-20.50	-17.14	-16.50	-46.38	-47.50
Angle of attack, α, deg	.00	1.00	.00	4.00	.00	.75	15.00	19.00	.00	1.00	30.00	30.50	.00	.25
Pitch angle, θ, deg	-15.00	-15.75	-15.00	-12.00	-18.30	-18.00	.00	4.25	-18.30	-19.50	15.00	14.00	-45.00	-47.25
Pitch angle error, θ_e, deg	.00	.00	.00	2.50	.00	.00	.00	3.00	.00	.50	.00	3.00	.00	.00
Roll angle, ϕ, deg	.00	.00	.00	.00	.00	1.25	.00	.00	.00	3.75	.00	.50	.00	.00
Yaw angle, Ψ, deg	.00	.00	.00	1.50	.00	.50	.00	-.50	.00	3.25	.00	.00	.00	2.50
Flight-path velocity, V, m/s	13.41	12.66	26.82	26.66	26.82	26.19	26.82	27.38	26.82	26.10	26.82	26.86	27.09	28.60
Vertical velocity, V_v, m/s	3.86	3.65	7.73	7.35	8.72	8.42	7.37	6.97	8.72	9.14	7.90	7.63	19.61	21.09
Horizontal velocity, V_h, m/s	12.84	12.13	25.68	25.63	25.36	24.80	25.79	26.47	25.36	24.45	25.63	25.76	18.69	19.32
Free-flight time, t, s	.15	.16	.07	.07	.07	.05	.07	.05	.07	.06	.07	.07	.07	.32
Umbilical separation time, t_u, s	1.00	No separation	1.00	1.00	.75	.78	.75	.77	.75	.77	.75	.62	.75	.74

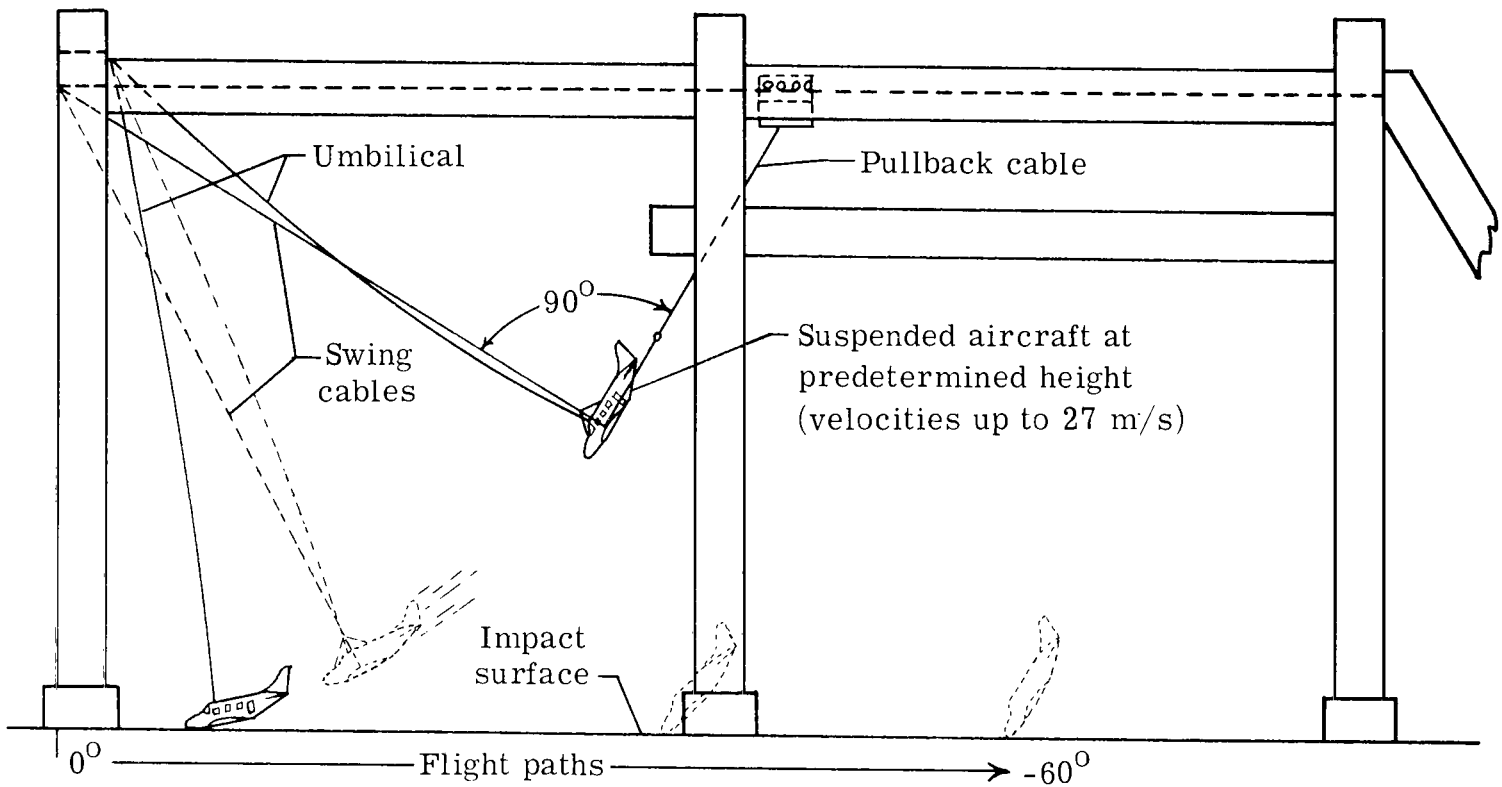

Figure 1.- Full-scale aircraft crash-test technique.

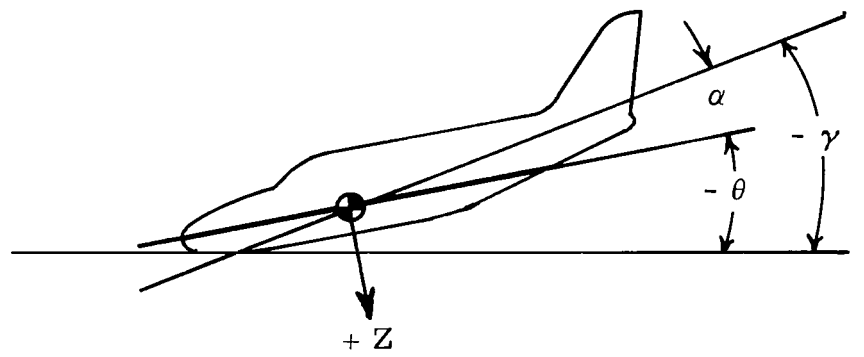

γ Flight-path angle
α Angle of attack
θ Pitch angle,
$\theta = \gamma + \alpha$

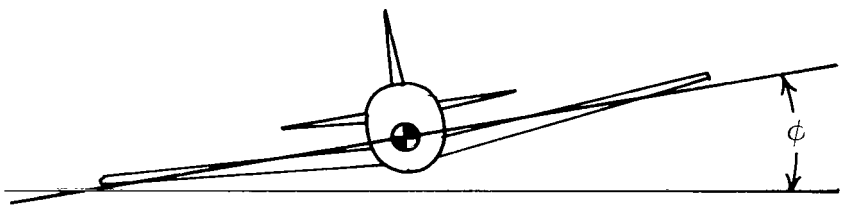

ϕ Roll angle

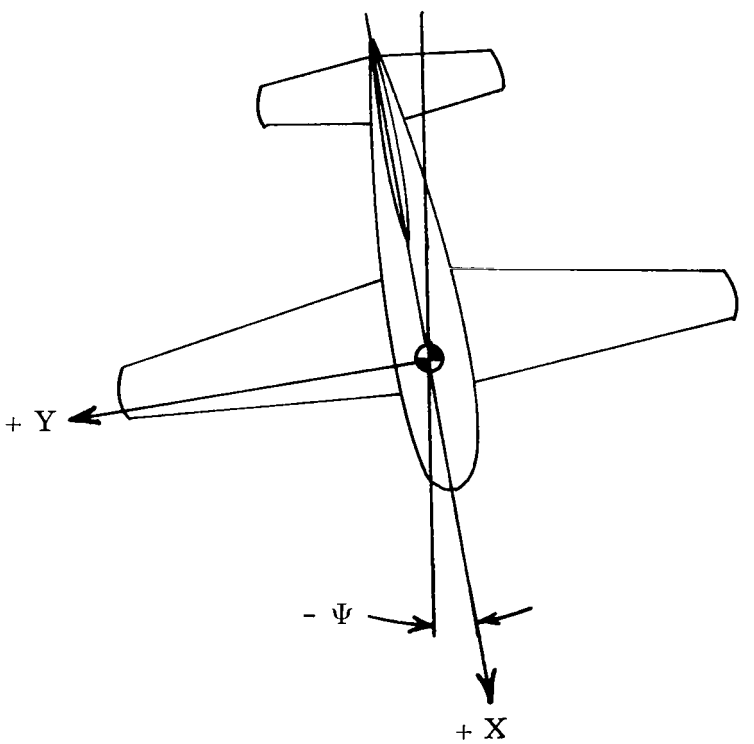

Ψ Yaw angle

Figure 2.- Sketches identifying flight path, crash attitude, axes, and force directions.

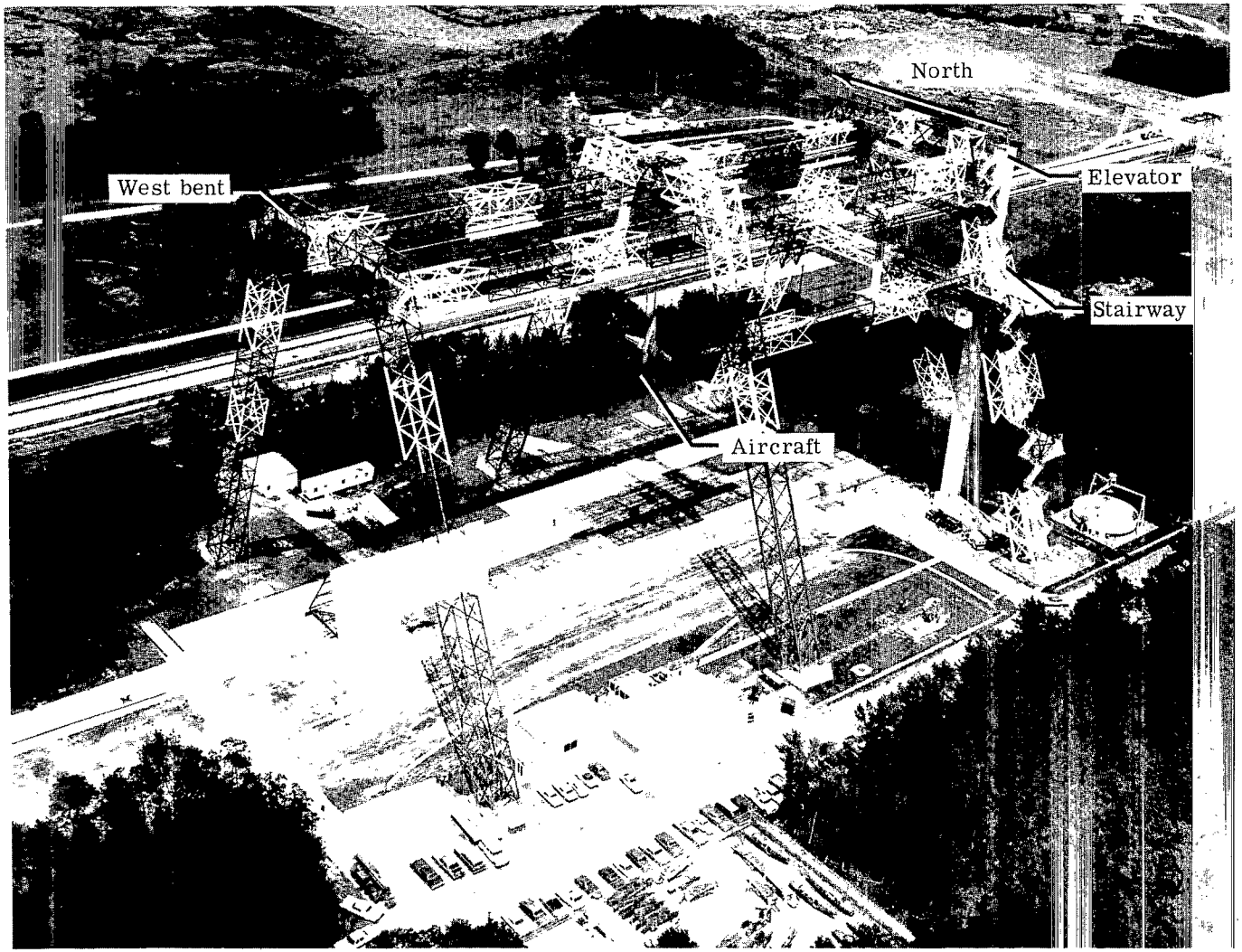

L-74-2505.1

Figure 3.- Impact dynamics research facility at Langley Research Center.

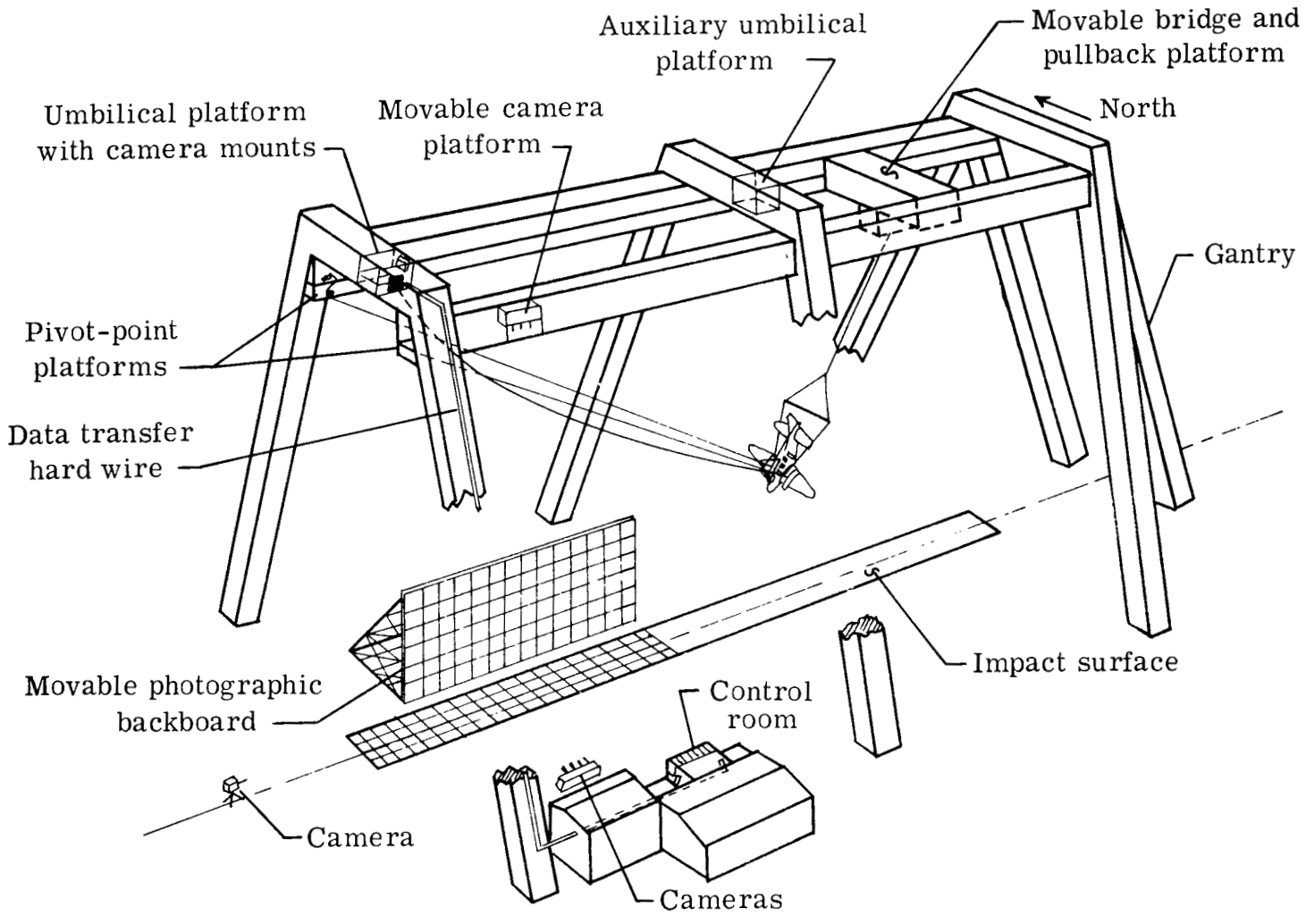

Figure 4.- Diagram of impact dynamics research facility.

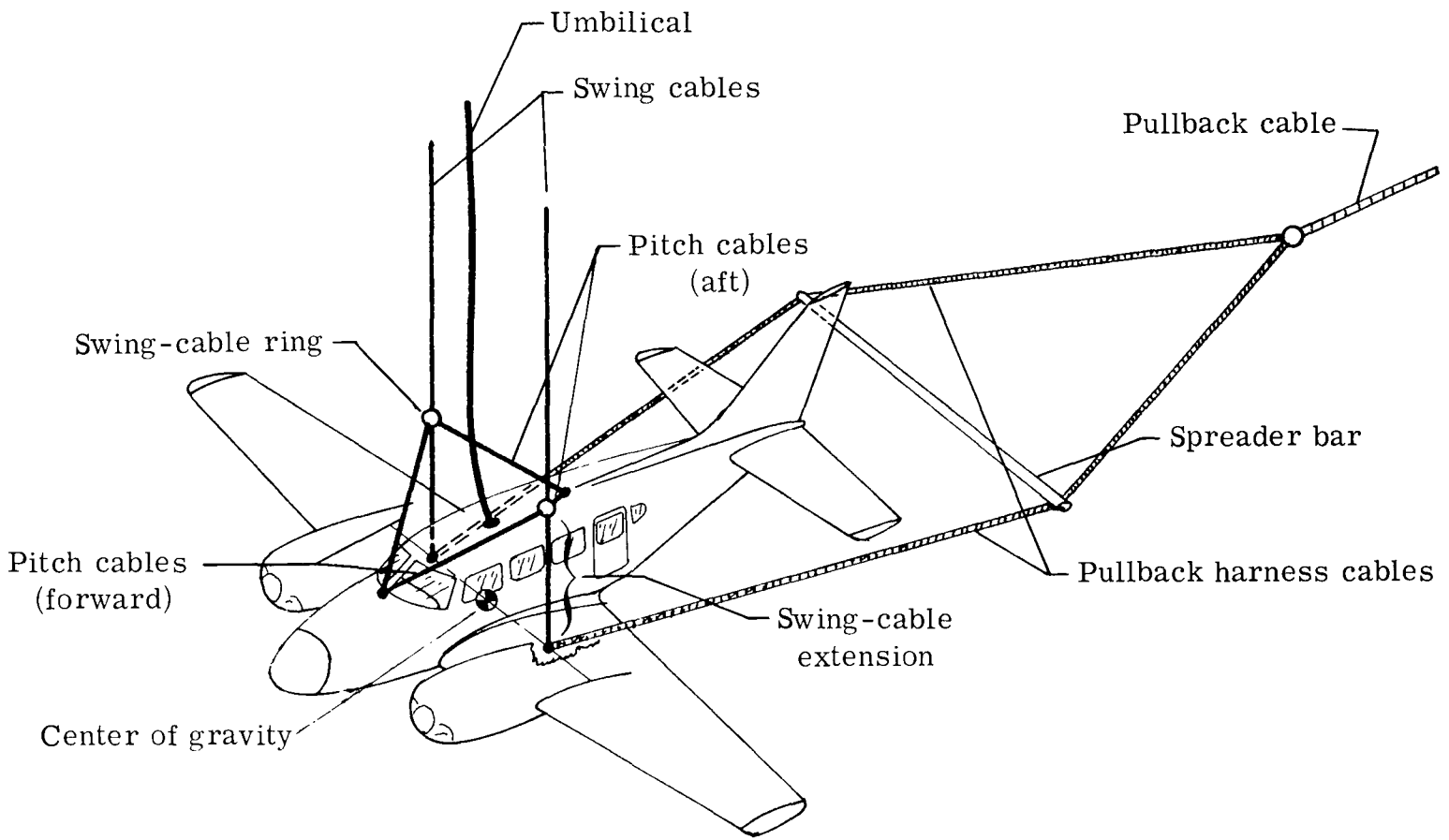

Figure 5.- Aircraft suspension system, swing harness refers to swing-cable extensions and pitch cables; pullback harness refers to pullback harness cables and spreader bar.

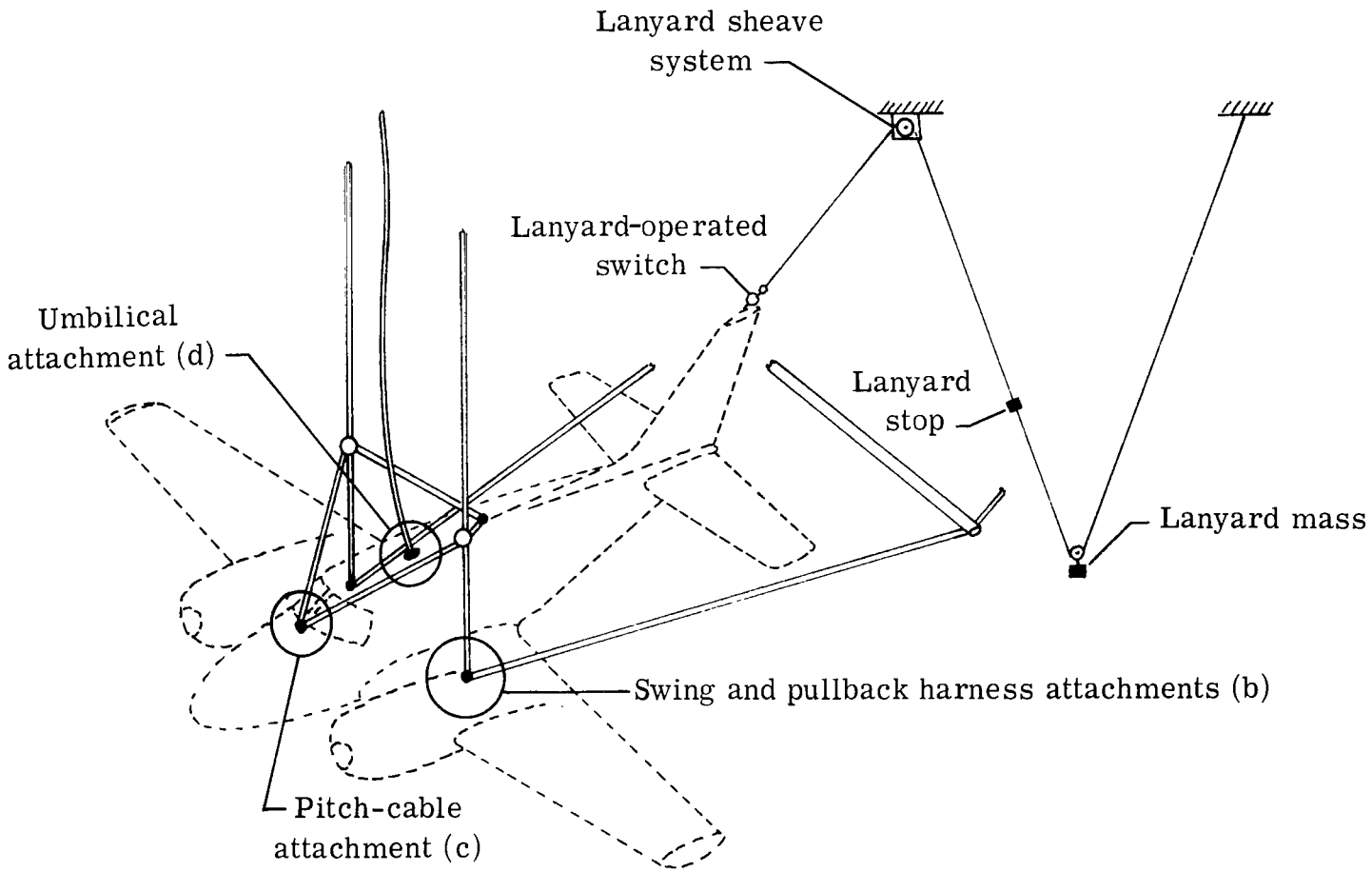

(a) System diagram.

Figure 6.- Aircraft release and separation systems.

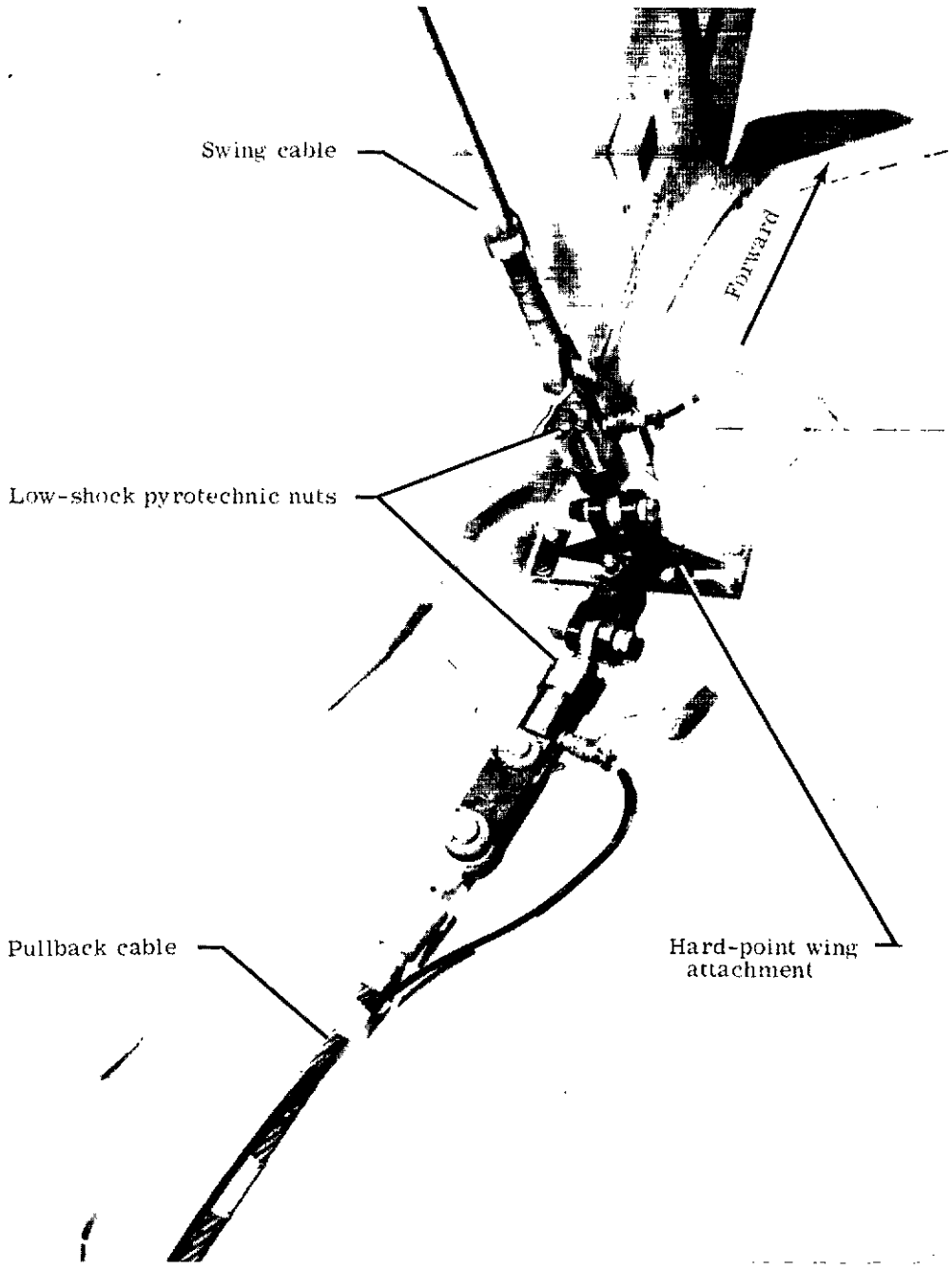

L-75-4653.1

(b) Aircraft swing and pullback harness attachment and pyrotechnic units.

Figure 6.- Continued.

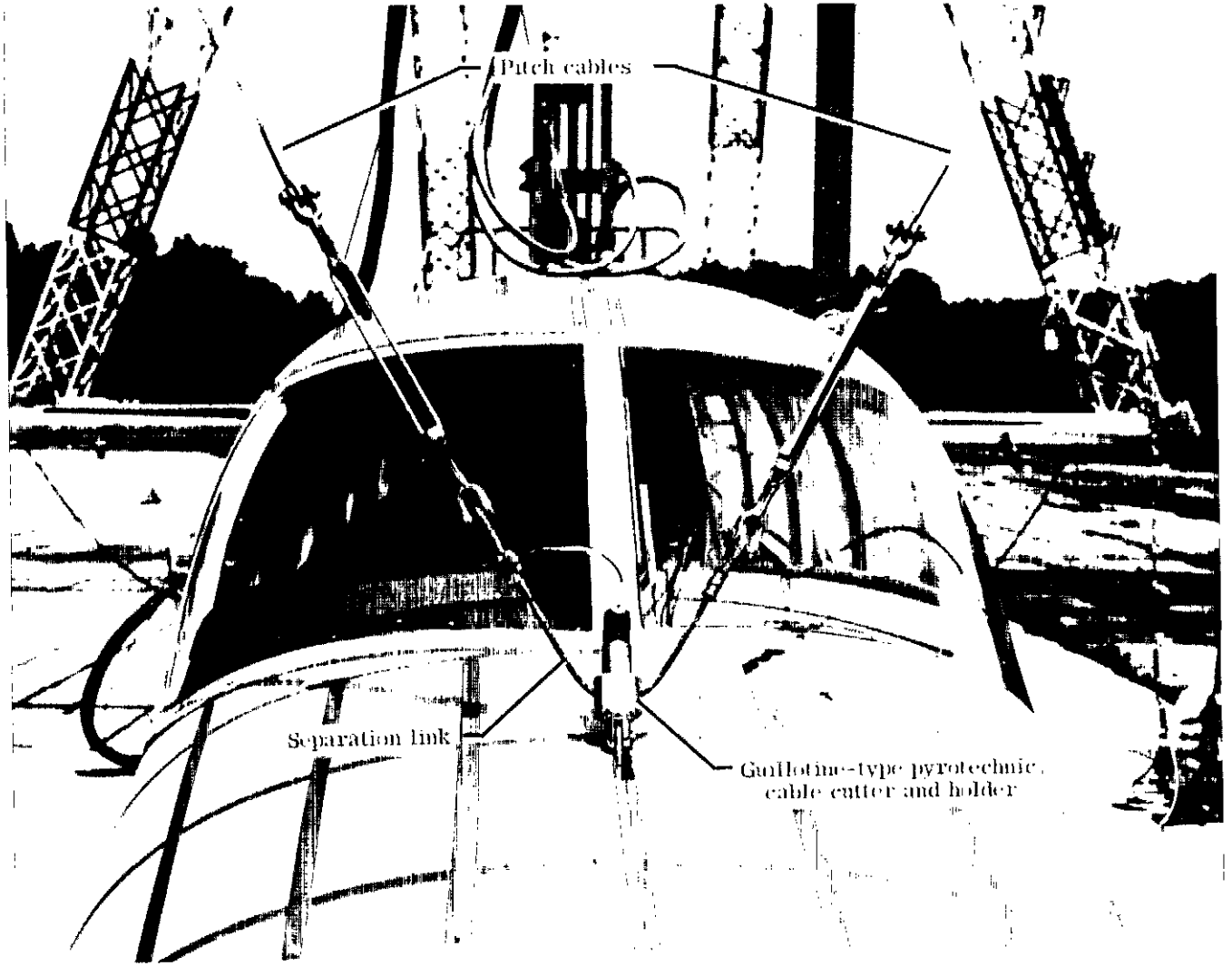

L-75-4654.1

(e) Aircraft pitch-cable attachment and pyrotechnic separation units.

Figure 6.- Continued.

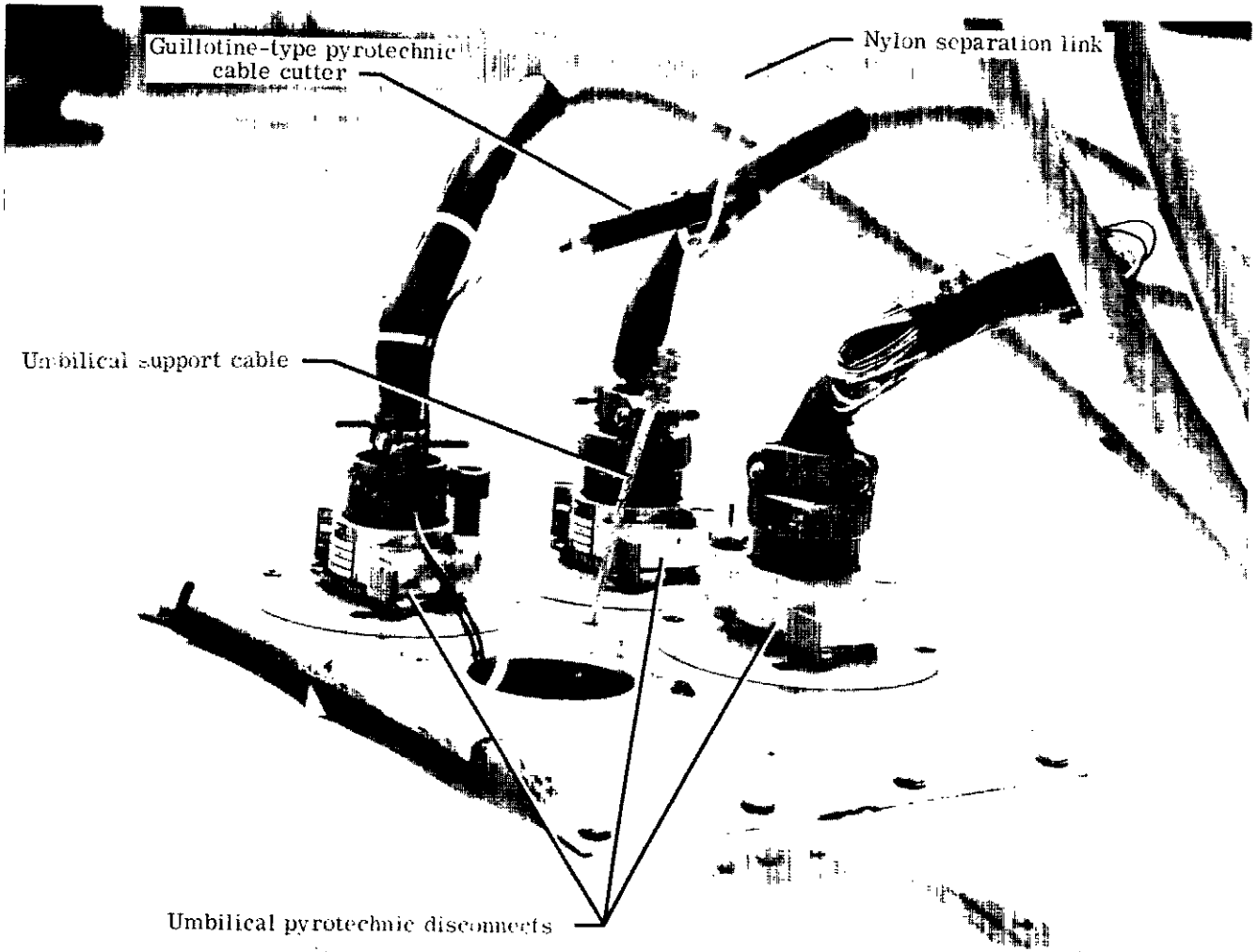

L-75-4660.1

(d) Aircraft umbilical cable attachment and pyrotechnic separation units.

Figure 6.- Concluded.

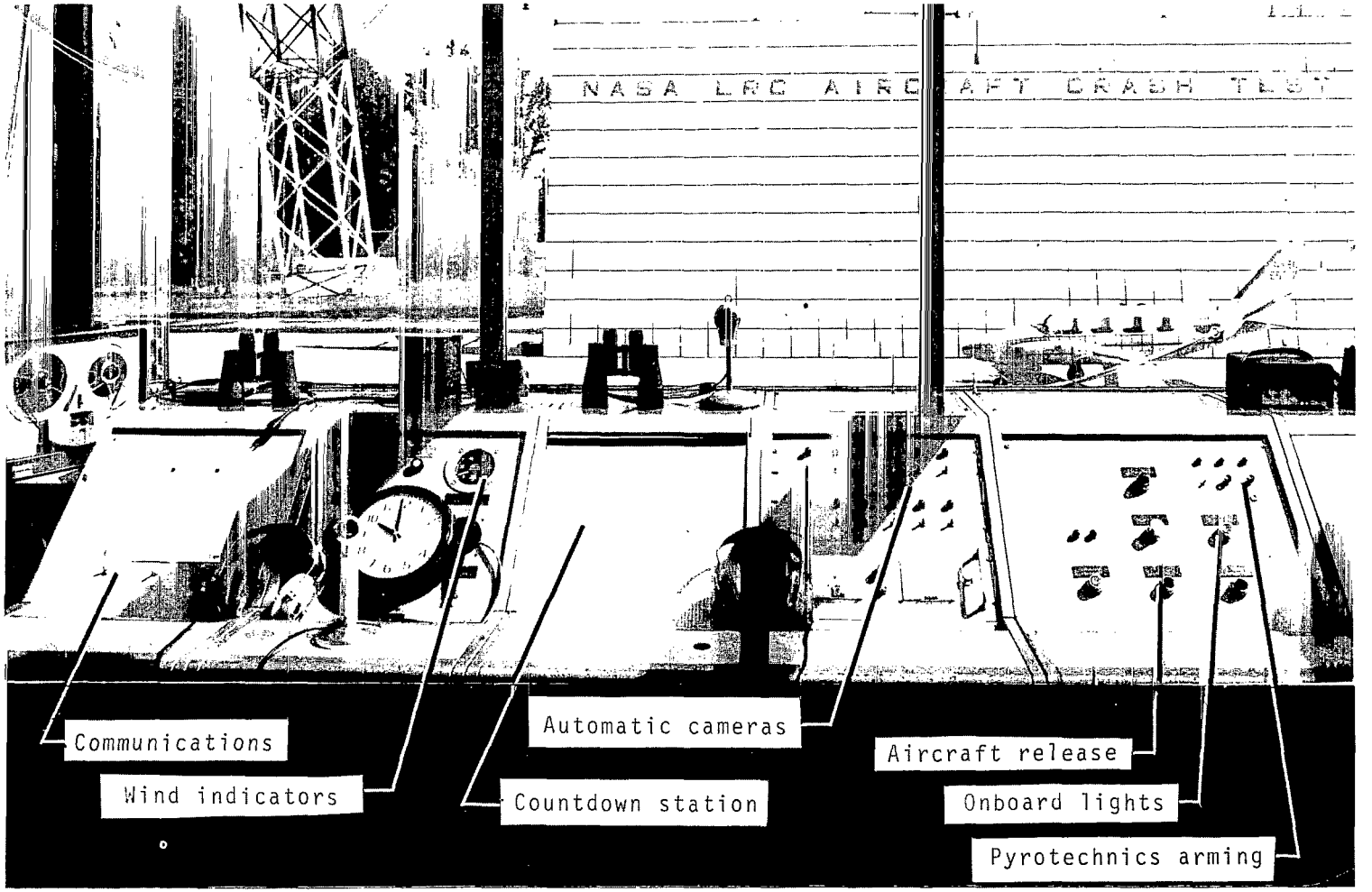

L-76-124

Figure 7.- Control room operation panel.

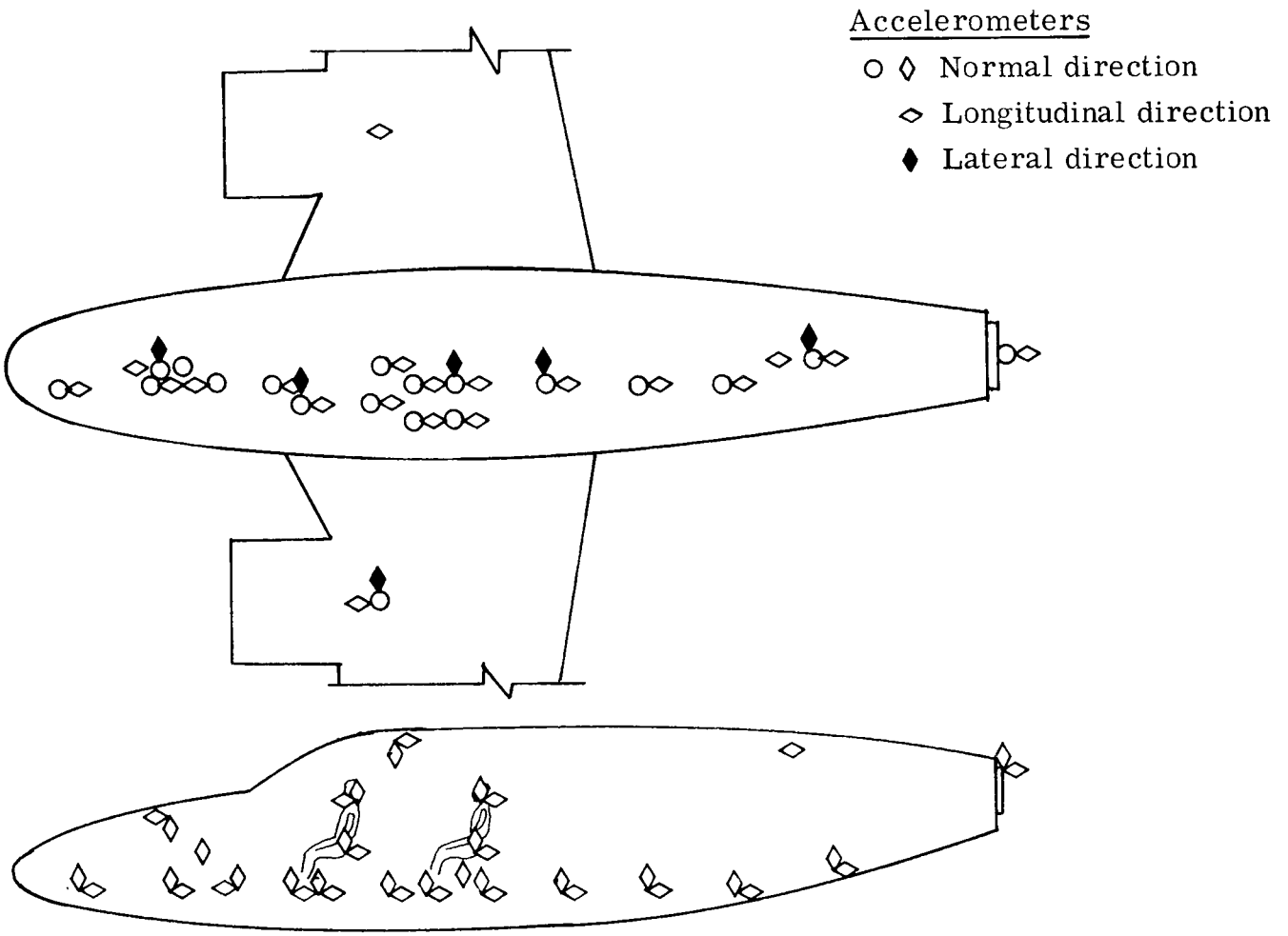

(a) Diagram showing typical accelerometer layout.

Figure 8.- Aircraft onboard data instrumentation.

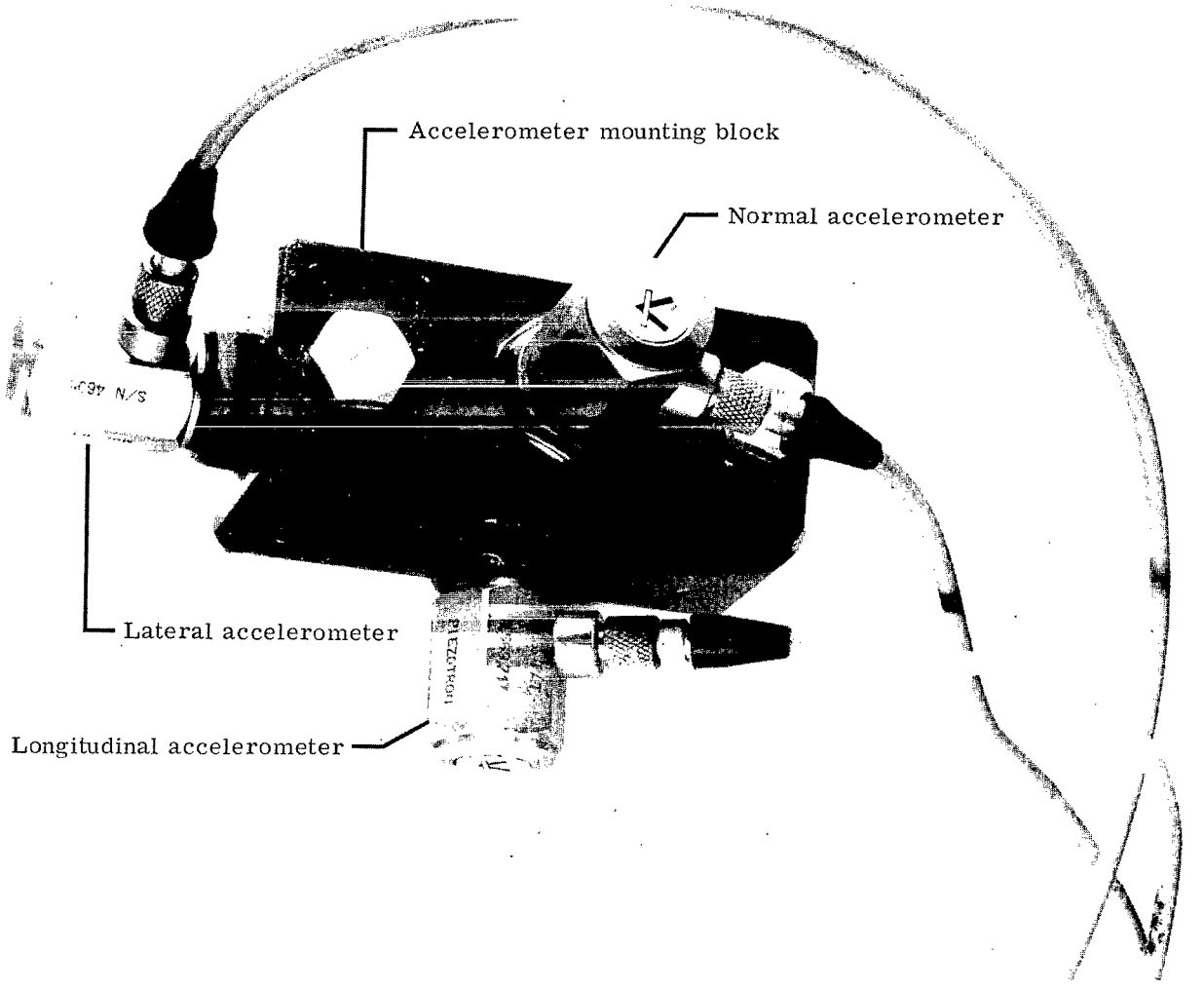

L-76-125

(b) Typical triaxial accelerometer installation.

Figure 8.- Concluded.

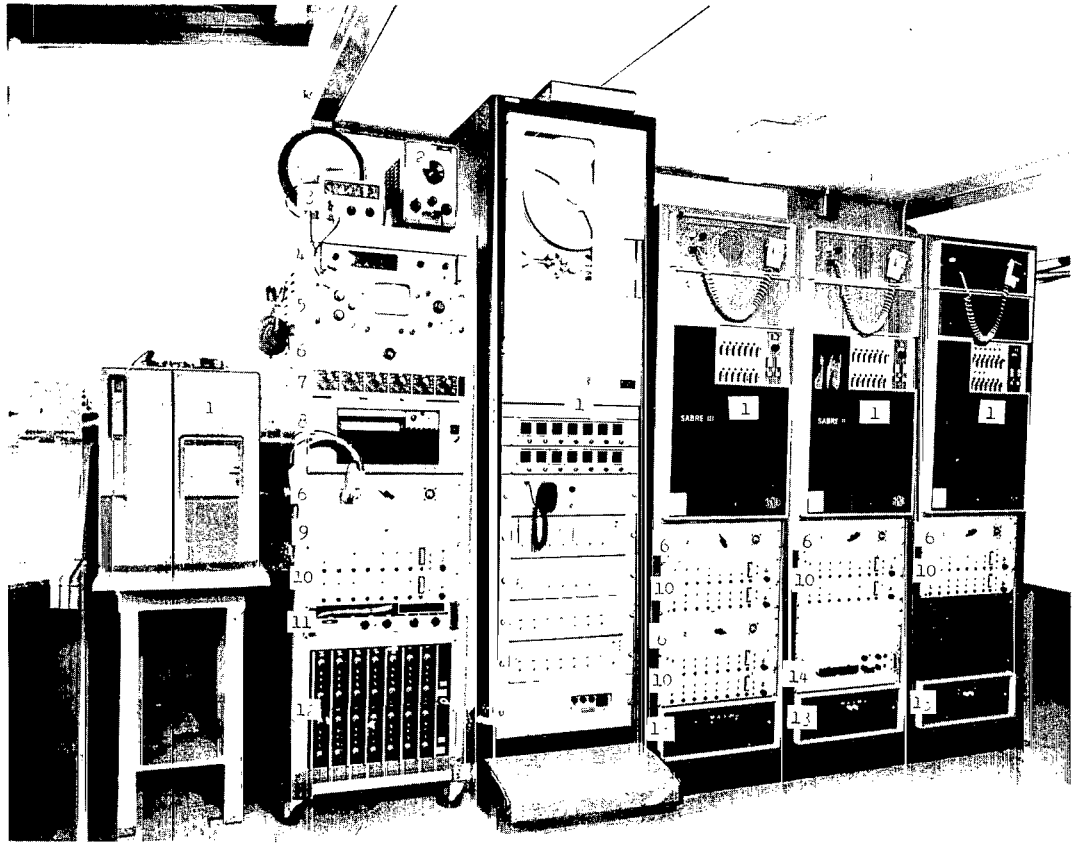

Equipment list

1. Tape recorder
2. Audio oscillator
3. Digital volt-ohm meter
4. Electronic counter
5. Oscilloscope
6. Tape recorder monitor switch
7. Galvanometer driver
8. Oscillograph
9. Tape recorder squelch unit
10. Accelerometer conditioning chassis
11. IRIG-A time code generator
12. Amplifiers
13. Tape recorder power supply
14. Strain-gage power supply

L-75-4656.1

Figure 9.- Control room data conditioning and recording equipment.

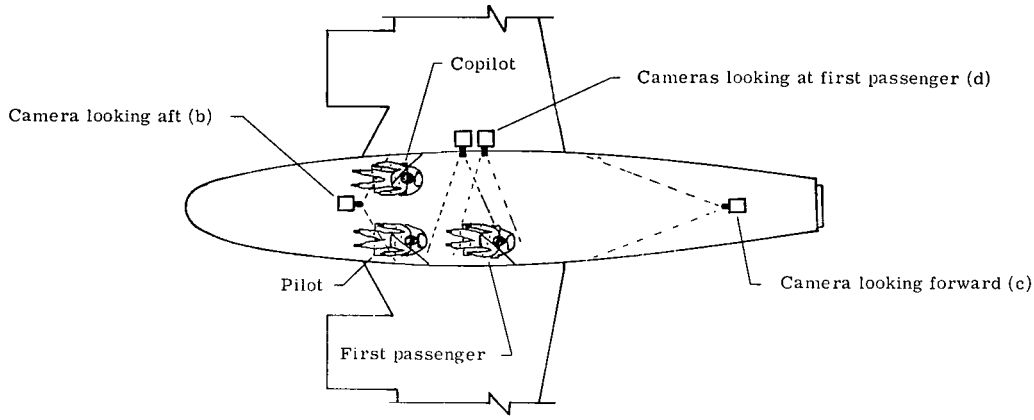

(a) Diagram of typical camera layout.

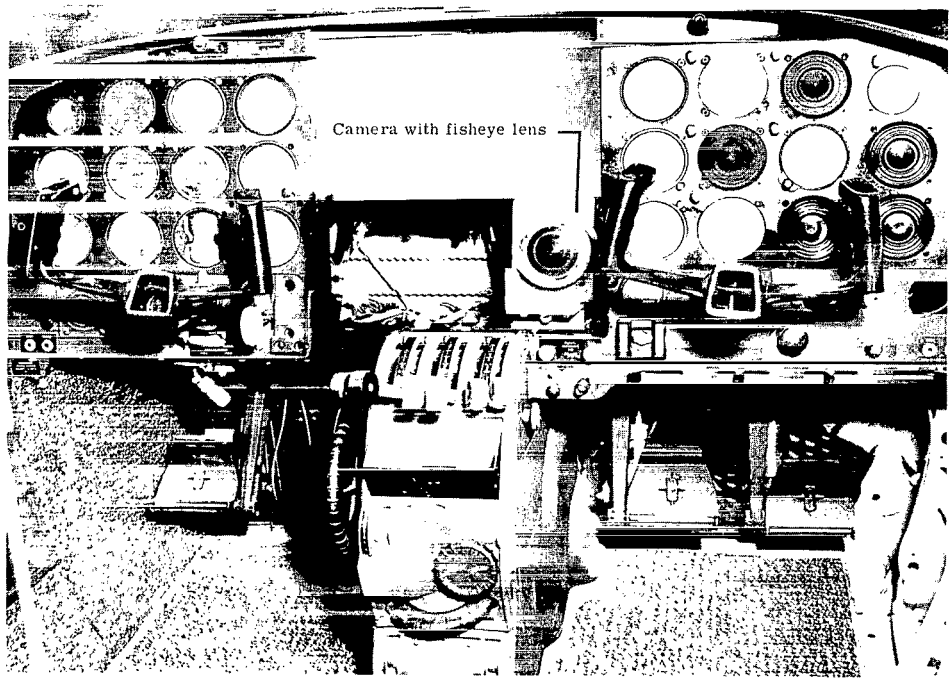

L-76-126

(b) Camera mounted in instrument panel, looking aft.

Figure 10.- Aircraft onboard camera coverage.

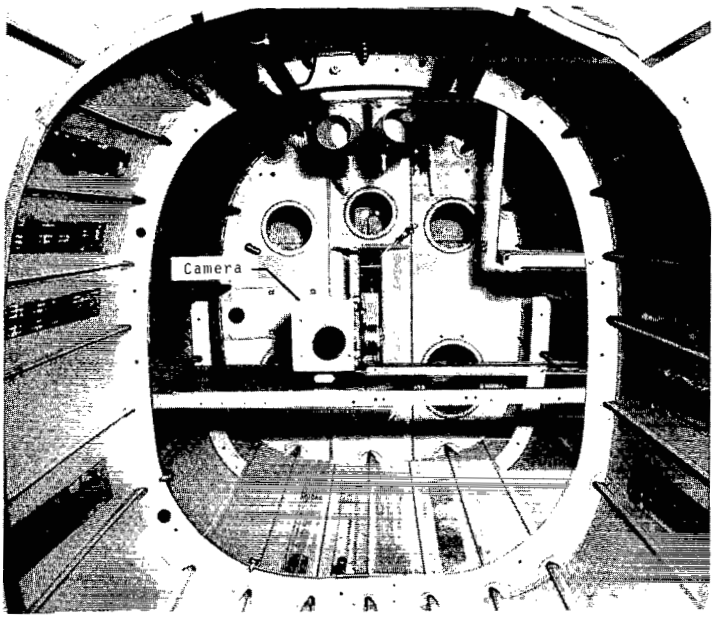

L-75-4659.1

(c) Camera located in rear of fuselage, looking forward.

L-75-4664

(d) Cameras mounted starboard to fuselage structure, looking at first passenger on port side of fuselage.

Figure 10.- Concluded.

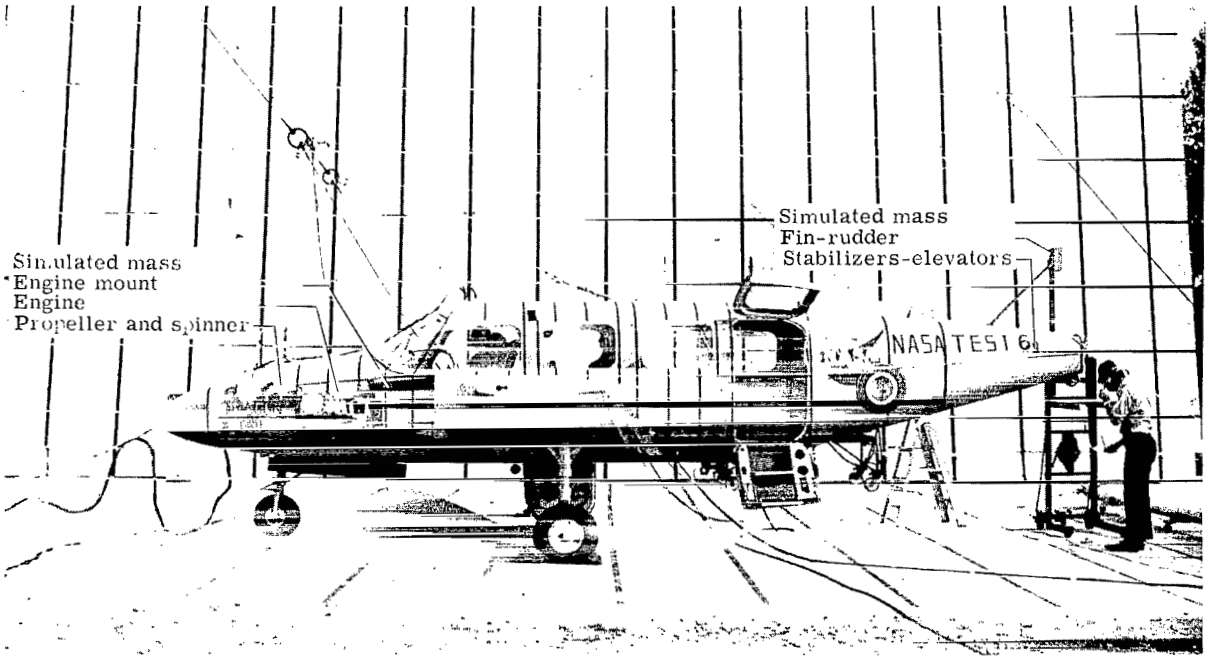

(a) Exterior view of stripped aircraft.

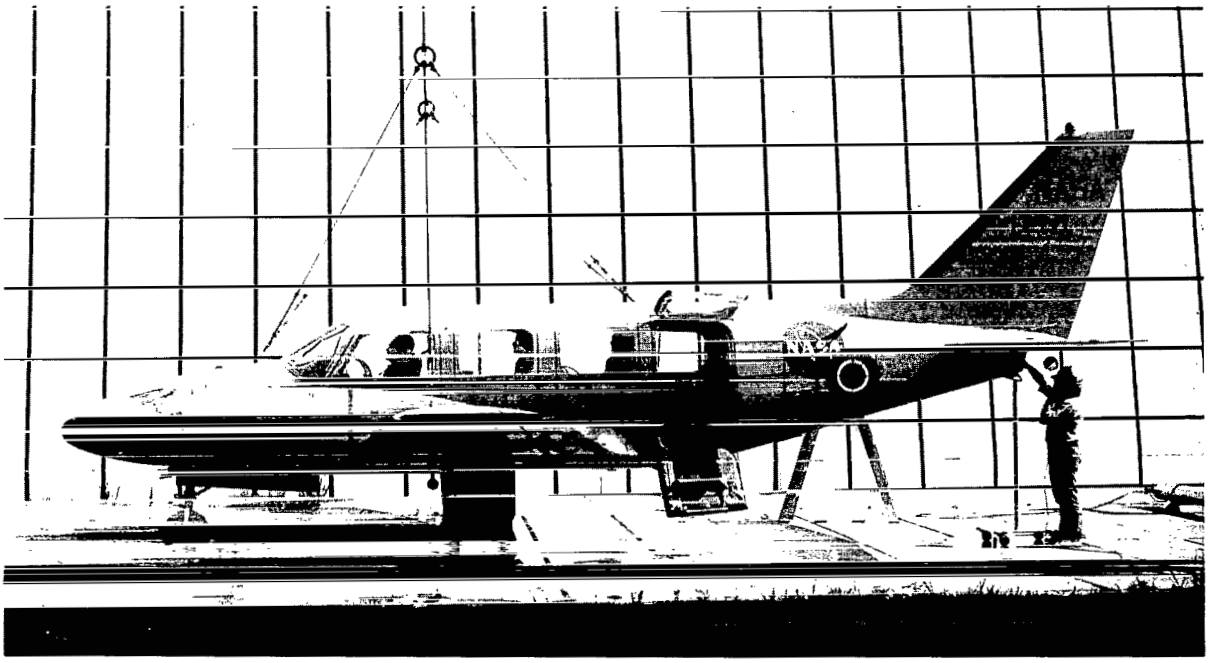

(b) Exterior view of complete aircraft. L-76-127

Figure 11.- Typical aircraft in crash-test preparation.

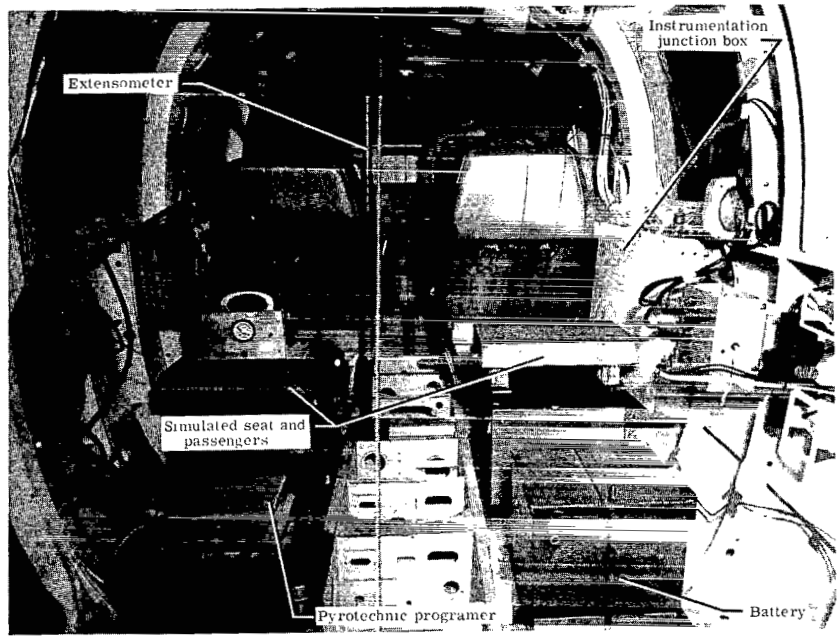

(c) Interior view of stripped aircraft.

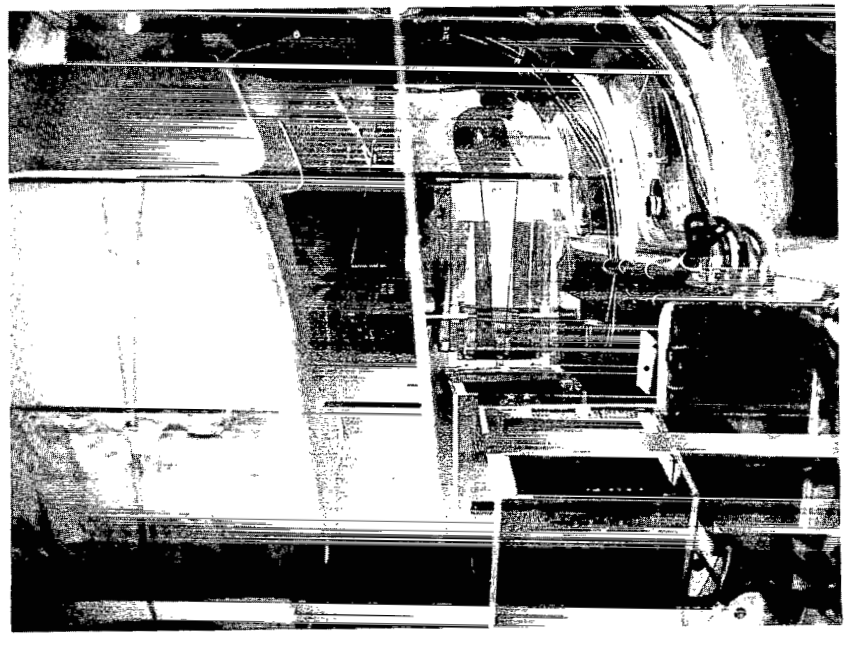

(d) Interior view of complete aircraft. L-76-128

Figure 11.- Concluded.

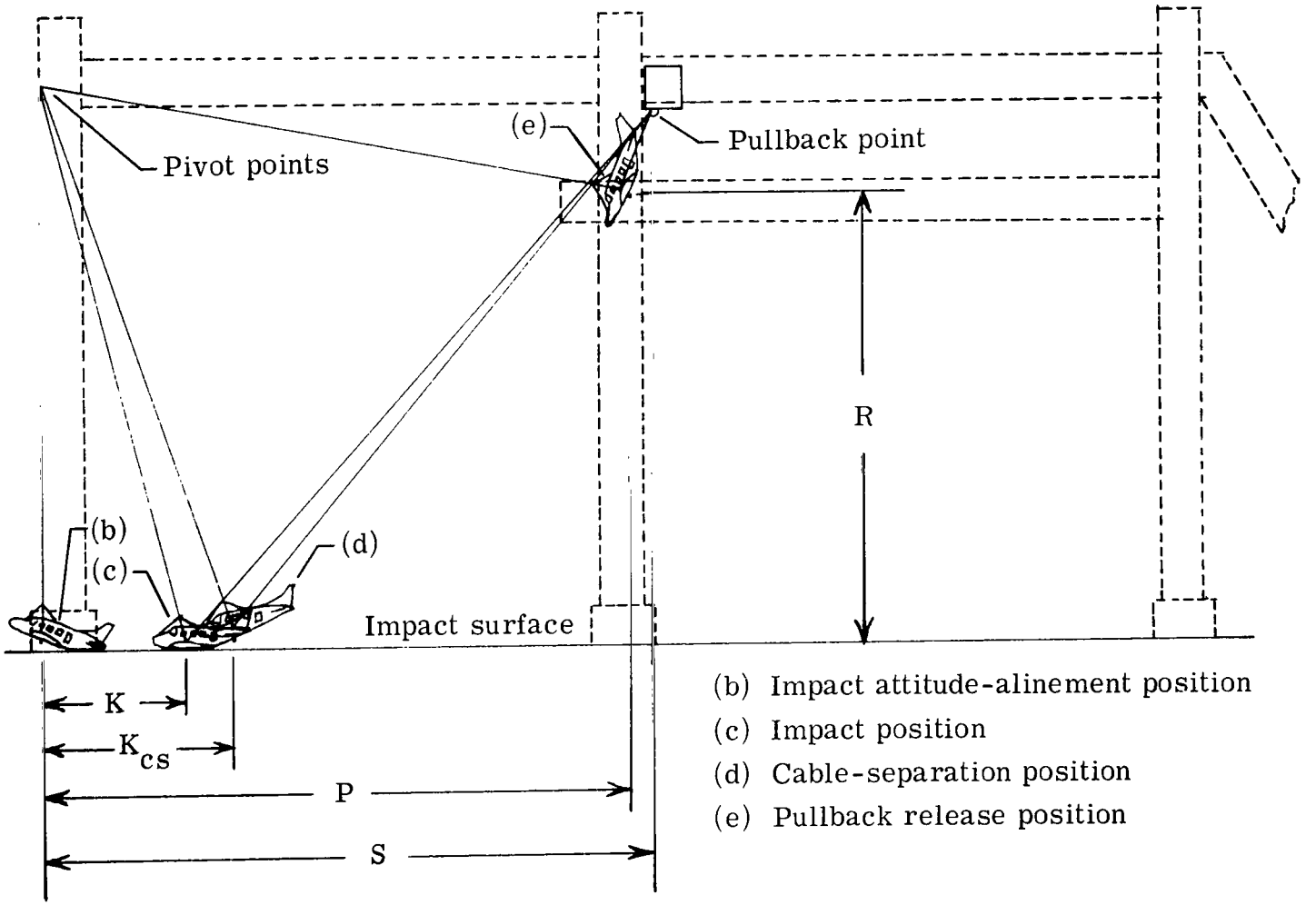

(a) Alinement positions diagram.

Figure 12.- Primary alinement positions for aircraft crash-test preparations.

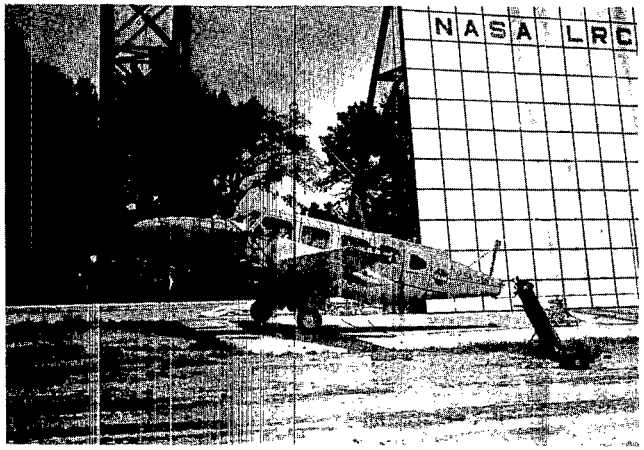

(b) Impact attitude-alinement position.

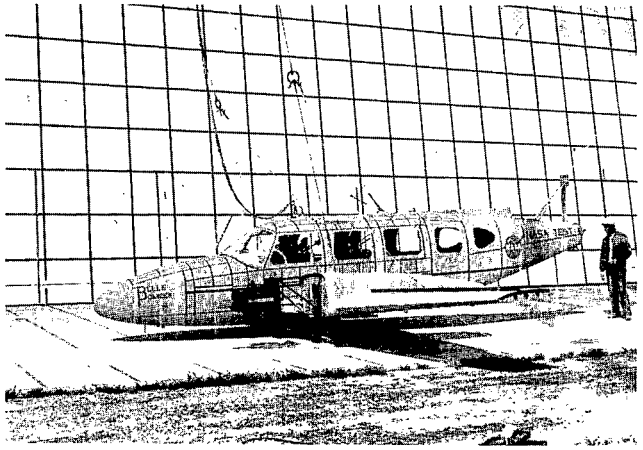

(c) Impact position.

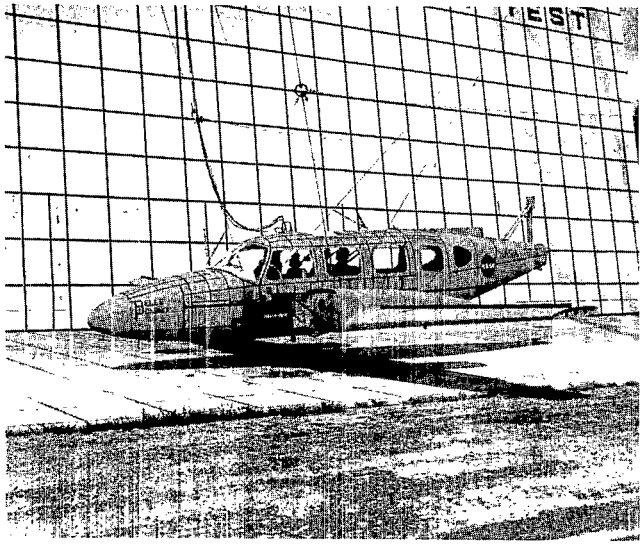

(d) Cable-separation position.

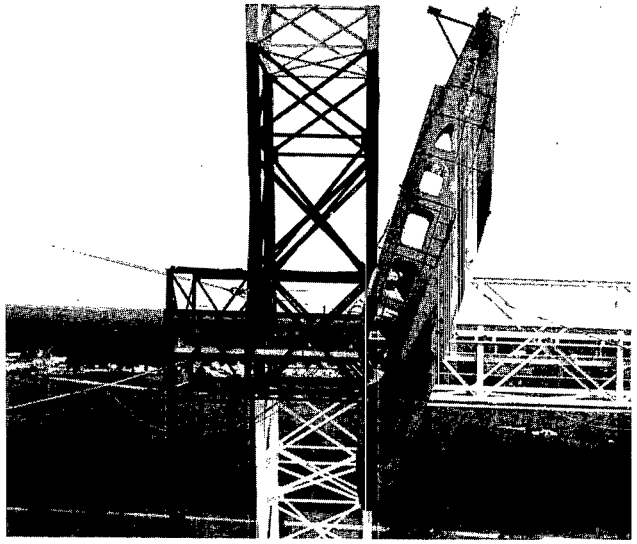

(e) Pullback release position.

Figure 12.- Concluded. L-76-129

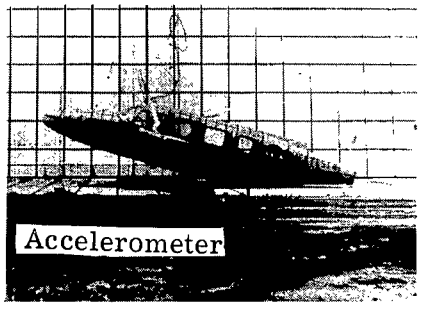

(a) Primary impact.

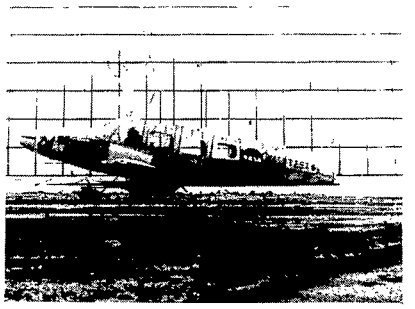

(b) 0.05 s after contact.

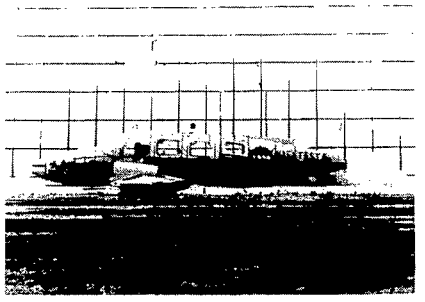

(c) 0.10 s after contact.

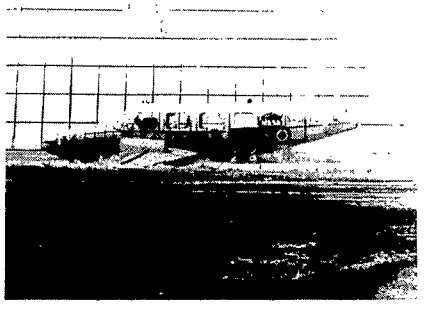

(d) 0.15 s after contact.

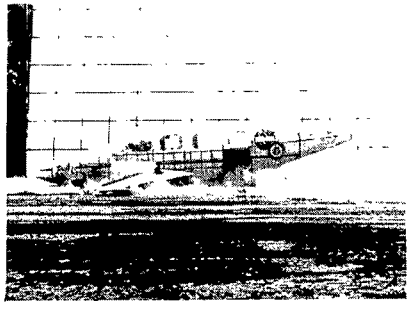

(e) 0.20 s after contact.

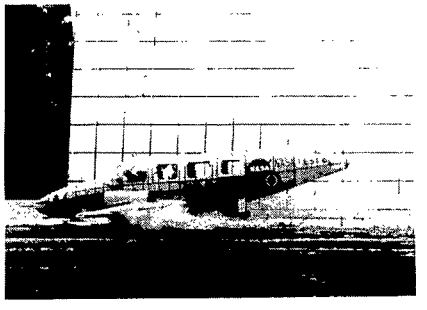

(f) 0.25 s after contact.

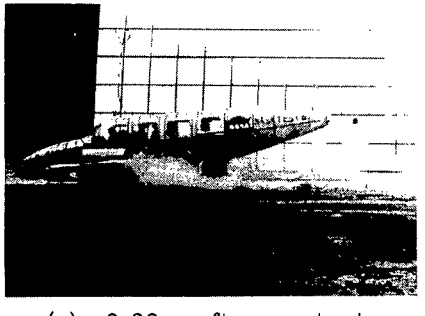

(g) 0.30 s after contact.

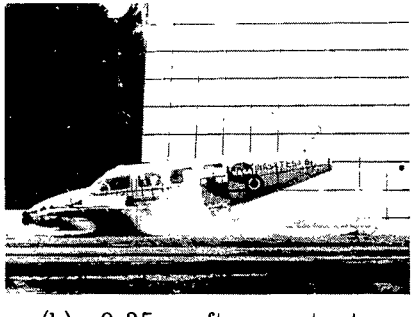

(h) 0.35 s after contact.

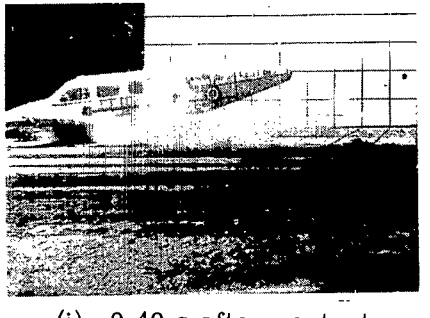

(i) 0.40 s after contact.

L-76-130

Figure 13.- Sequence photographs showing a typical aircraft crash test. $\gamma = -16.5^{o}$; $\theta = 14.0^{o}$; $\alpha = 30.5^{o}$.

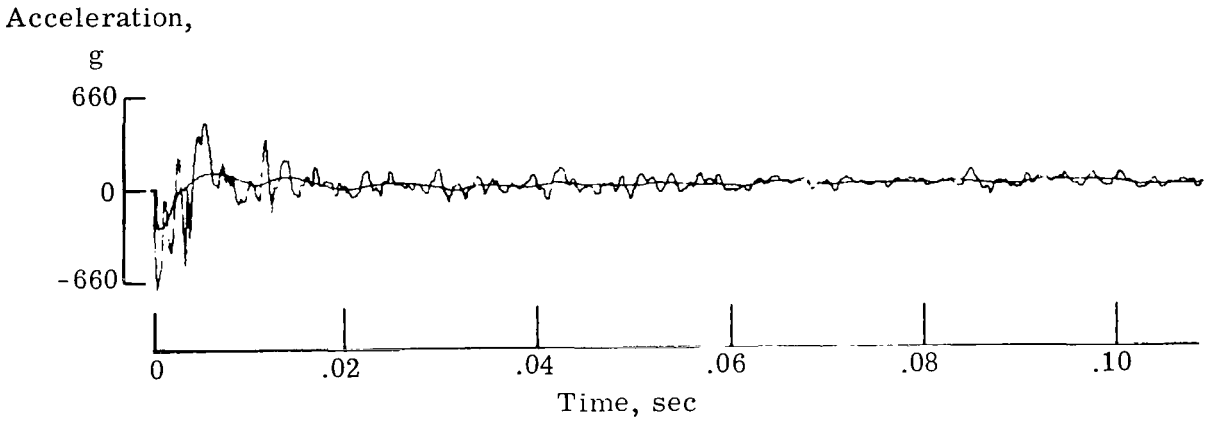

(a) Raw digitized acceleration trace with least-squares fit trace superimposed.

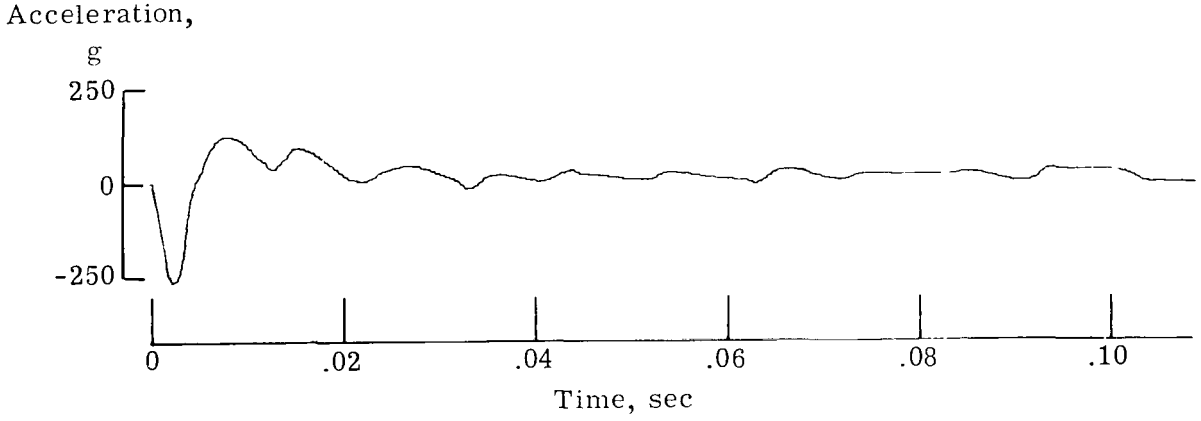

(b) Least-squares fit trace, expanded scale.

Figure 14.- Typical vertical acceleration time-history traces obtained during aircraft crash test.

(a) Camera in instrument panel.

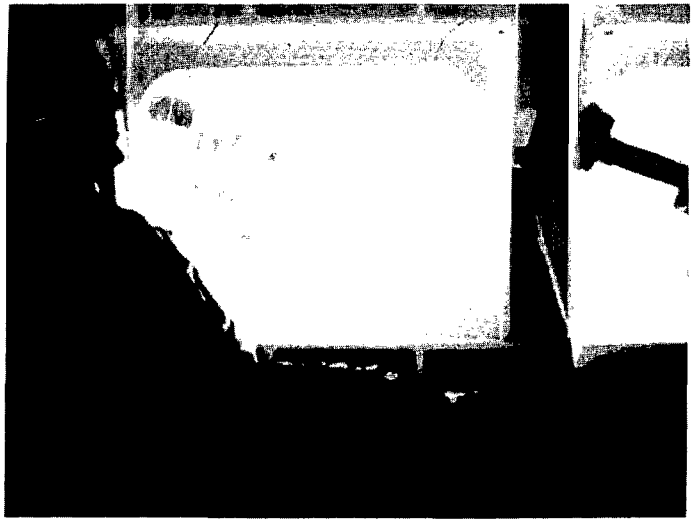

(b) Camera on fuselage exterior.

(c) Camera in aft end of fuselage.

L-76-131

Figure 15.- Onboard photographs taken during aircraft crash test.

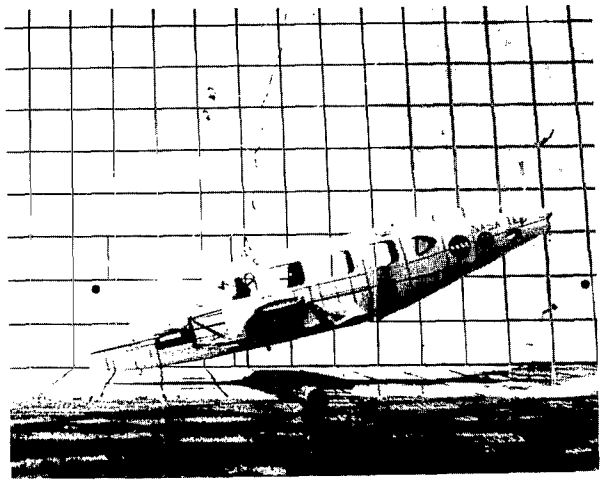

(a) Crash test 2, $\theta = -12^{o}$.

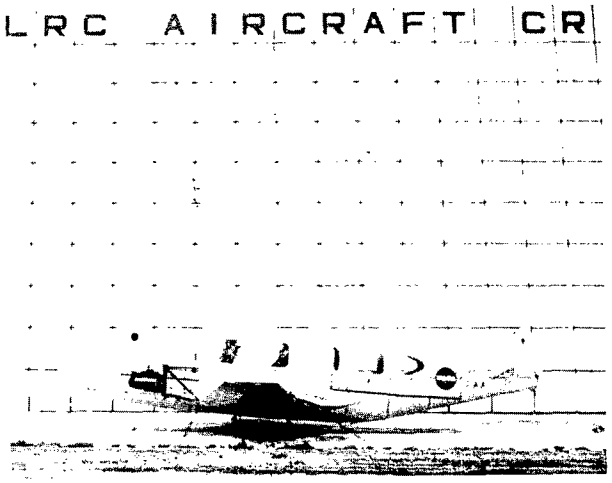

(b) Crash test 4, $\theta = 4.25^{o}$.

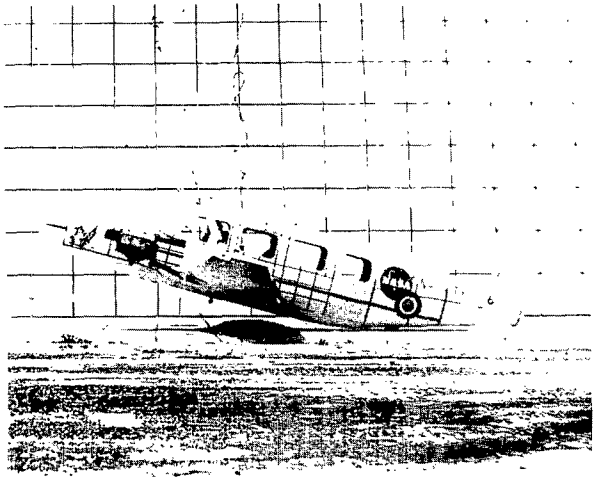

(c) Crash test 6, $\theta = 14^{o}$.

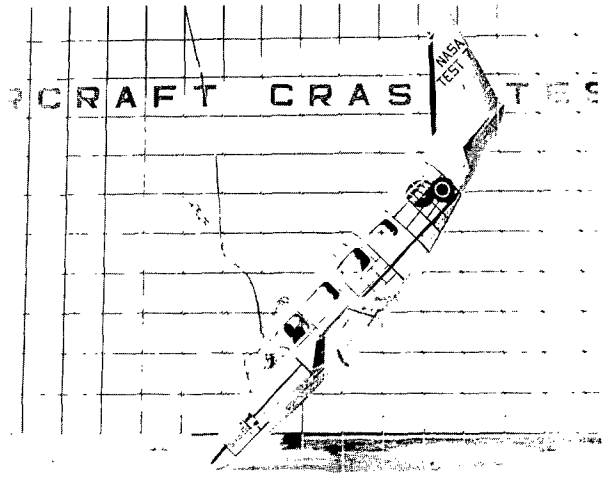

(d) Crash test 7, $\theta = -47.25^{o}$.

L-76-132

Figure 16.- Photograph showing aircraft crash attitudes for four crash tests.

APPENDIX A

DEFINITIONS AND EQUATIONS FOR AIRCRAFT CRASH-TEST GEOMETRY AND PERFORMANCE ANALYSIS OF THE IMPACT DYNAMICS RESEARCH FACILITY

General Description

For a given set of planned aircraft crash-test parameters within the physical limits of the facility, the test geometry necessary to set up the aircraft and facility to meet the parameters can be calculated using the equations in this section. The planned crash-test parameters consist of two types: the selected parameters and the calculated parameters. The selected parameters are those necessary to determine the test geometry of the aircraft-facility configuration and to represent the minimum requirement. The selected parameters are:

V	aircraft velocity along the flight path, degrees
α	angle of attack, degrees
γ	flight-path angle, degrees
θ	pitch angle, degrees
ϕ	roll angle, degrees
Ψ	yaw angle, degrees

The calculated parameters are those determined by the equations based on the selected parameters.

The equations and measurements are presented in the order in which they are used to determine the geometry. A sketch of the integral aircraft-facility geometric relation on which the equations are based is given in figure A1(a) for two positions of the aircraft. The impact position is shown with the aircraft fuselage in contact with the impact surface. The attitude of the aircraft with respect to the impact surface and pivot points is set by the selected parameters and is the attitude of the aircraft at impact. The impact position is fixed by the dimensions B and K. Distance B is measured from a scaled drawing of the aircraft configuration as shown in figure A2. Distance K is the calculated distance from the pivot points to the aircraft target. The target is located directly under the

center of gravity of the aircraft (see fig. A3) and as close to the fuselage as possible. The impact point, that point on the impact surface where the aircraft fuselage impacts, is represented by dimension F.

The pullback release position is the location of the aircraft relative to the impact surface, pivot points, and pullback point where the aircraft starts the swing phase of the test. The position is fixed by the calculated dimensions P and R. The location of the pullback point necessary to establish an angle of 90^{o} between the swing and pullback cables is given by dimension S.

The location of the aircraft in the cable-separation position, that position at which the swing cables are separated from the aircraft and the aircraft goes into free-flight mode, is fixed by dimensions B_{cs} and K_{cs} as shown in figure A1(b).

The test geometry is demonstrated with the use of an aircraft with retracted landing gear. For aircraft with extended landing gear, all equations are the same; however, the landing gear wheel becomes the aircraft impact point.

Equations and Measurements for Facility and Aircraft Pretest Setup

Angles are positive in all equations involving trigonometric functions. The equations and measurements are presented in the order in which they are used to determine the geometry.

A	Vertical distance from impact surface to pivot points, m	66.495
B	Vertical distance from impact surface to aircraft c.g. in impact position, m (see fig. A2)	Measured
C	Length of swing cables, m	$C = \frac{A - B}{\cos \gamma}$
D	Horizontal distance from pivot points to aircraft c.g. in impact position, m	$D = (A - B) \tan \gamma$
E	Horizontal distance from impact point to aircraft c.g. in impact position, m (negative for positive pitch angles) (see fig. A2)	Measured
F	Horizontal distance from pivot points to impact point, m	F = D - E
G	Normal distance from bottom of aircraft fuselage to aircraft c.g., m (see fig. A3)	Measured
H	Normal distance from bottom of fuselage to center of alinement target, m (see fig. A3)	Measured

I	Normal distance from alinement target to aircraft c.g., m	$I = G + H$
J	Horizontal distance from aircraft c.g. to alinement target with aircraft in impact position, m	$J = I \sin \theta$
K	Horizontal distance from pivot points to alinement target with aircraft in impact position, m	$K = D + J$
L	Experimentally determined value for estimating aircraft and swing-cable drag correction (see fig. A4)	Measured
g	Acceleration due to gravity, m/s^2	9.815
M	Vertical distance from impact surface to aircraft c.g. in pullback release position, m	$M = B + \frac{V^2}{2g}(1 + L)$
β	Angle of swing cables with aircraft in pullback release position with respect to vertical reference, deg	$\beta = \text{Arc cos} \frac{A - M}{C}$
N	Horizontal distance from pivot points to aircraft c.g. in pullback release position, m	$N = C \sin \beta$
O	Horizontal distance from aircraft c.g. to alinement target with aircraft in pullback release position, m	$O = I \sin (\beta - \alpha)$
P	Horizontal distance from pivot points to aircraft alinement target with aircraft in pullback release position, m	$P = N + O$
Q	Vertical distance from alinement target to aircraft c.g. in pullback release position, m	$Q = I \cos (\beta - \alpha)$
R	Vertical distance from impact surface to alinement target with aircraft in pullback release position, m	$R = M - Q$
S	Horizontal distance from pivot points to pullback point, m	$S = \frac{C}{\sin \beta} - \frac{1.58}{\tan \beta}$
B_{cs}	Vertical distance from impact surface to aircraft c.g. in cable-separation position, m	$B_{cs} = B + 2 \sin \gamma$
γ_{cs}	Flight-path angle of aircraft in cable-separation position, deg	$\gamma_{cs} = \text{Arc cos} \frac{A - B_{cs}}{C}$
D_{cs}	Horizontal distance from pivot points to aircraft c.g. in cable-separation position, deg	$D_{cs} = \left(A - B_{cs}\right) \tan \gamma_{cs}$

APPENDIX A

θ_{cs}	Pitch angle of aircraft in cable-separation position, deg	$\theta_{cs} = \gamma_{cs} + \alpha$
J_{cs}	Horizontal distance from aircraft c.g. to alinement target with aircraft in cable-separation position, m	$J_{cs} = I \sin \theta_{cs}$
K_{cs}	Horizontal distance from pivot points to alinement target with aircraft in cable-separation position, m	$K_{cs} = D_{cs} + J_{cs}$

Definition and Equations for Planned Aircraft Crash-Test Parameters (Table AI)

V_v	Vertical velocity (sink speed) of aircraft at impact, m/s	$V_v = V \sin \gamma_{cs}$
V_h	Horizontal velocity of aircraft at impact, m/s	$V_h = V \cos \gamma_{cs}$
T	Aircraft free-flight distance along flight path, m	2.0
t	Aircraft free-flight time between cable separation and impact, s	$t = \frac{T \sin \gamma_{cs}}{V_v}$
V_ω	Pitching velocity of aircraft around c.g. at impact, rad/s	$V_\omega = \frac{\pi(\theta - \theta_{cs})}{180t}$
t_u	Umbilical separation time, elapsed time between swing-cable separation and umbilical separation, s	Regulated

FACILITY PERFORMANCE ANALYSIS

Measurements and Equations

The measure of performance of the impact dynamics research facility (IDRF) is the accuracy with which the planned aircraft crash-test parameters are met during a test. The planned and actual parameters obtained during seven aircraft crash tests are presented in table AI. The actual parameters are determined by using the equations and measurements listed below.

The parameters that are obtained by measurement from the motion-picture film and recorded data are γ_{cs}, θ_{cs}, θ_a, ϕ, Ψ, V_h, t, and t_u. All other parameters are calculated from the measured parameters as follows:

θ_a	Actual pitch angle of aircraft at impact, deg	Measured
α_a	Actual angle of attack of aircraft at impact, deg	$\alpha_a = \theta_a - \gamma_{cs}$
θ_e	Pitch angle error due to catenary effect, deg	$\theta_e = \theta_{cs} - (\gamma_{cs} + \alpha)$

APPENDIX A

V	Actual velocity of aircraft along flight path at impact, m/s	$V = \frac{V_h}{\cos \gamma_{cs}}$
V_v	Actual vertical velocity at impact, m/s	$V_v = V_h \tan \gamma_{cs}$
V_ω	Pitching velocity of aircraft around c.g. at impact, rad/s	$V_\omega = \frac{\pi(\theta_a - \theta_{cs})}{180t}$

The first aircraft (crash test 1) was crash tested with landing gear retracted at a velocity of 12.66 m/s along a flight path of -16.75^o and a pitch angle of -15.75^o. The wind velocity was variable up to 4.5 m/s out of the west. All test parameters were close to those selected, with aircraft velocity along the flight path showing the largest error (about 6 percent). All systems except the umbilical separation functioned properly. The umbilical did not separate because the pyrotechnic battery discharged when the pyrotechnic circuit was shorted by part of the damaged aircraft structure.

Crash tests 2, 4, 6, and 7 were performed with the landing gear retracted at flight-path velocities of approximately 27.0 m/s. Figure A5 shows photographs of each of these test aircraft just before the aircraft contacted the impact surface. The flight paths were within 6 percent of that expected and the velocities along the flight paths were accurate within 6 percent.

Tests 3 and 5 were performed with the landing gears extended. The test geometry for these tests was designed on the basis that the aircraft fuselage would contact the ground at the same location as in test 2. The flight-path angles were set higher than for test 2 to obtain swing-cable separations before the landing gear made contact with the impact surface. The flight-path angles for tests 3 and 5 were accurate within 8 percent of the planned angles and the pitch angles were within 6 percent of the planned angles. The pitch angle θ_a varied as much as 4.25^o from the selected values for the seven tests. The greater part of these errors resulted from the cable catenary effect on the aircraft during the swing phase of the test. The manner in which the aircraft was affected by the cable catenary is illustrated by the sketch in figure A6. The positions of the aircraft and the swing cables, assuming no catenary, are shown by the dashed lines. The positions of the aircraft and swing cables with the cable catenary are shown by the solid lines. During the swing phase of the test, the aircraft oscillates in pitch during its travel along the swing arc because of the oscillating action of the swing cables. The error in pitch angle θ_e at impact is approximated by the following equation:

$$\theta_e = \theta_{cs} - (\gamma_{cs} + \alpha)$$

where θ_{cs} is the aircraft pitch angle at cable separation, γ_{cs} is the flight-path angle at cable separation, and α is the selected angle of attack. (See table AI.) The greatest error observed as a result of catenary effect occurred during tests 4 and 6 and measured approximately 3.0^{o}. Another error of less than 1.0^{o} is reflected in the pitch angle. This error was caused by a deviation from the calculated angular rotation of the aircraft in free flight.

There are two restoring forces which tend to alleviate the catenary effect. One is the centrifugal force generated as the aircraft swings toward the impact surface (up to 2g for the tests shown in table AI). The second force is the aircraft drag developed during the swing phase. This force is shown in table AI by the small pitch angle error θ_e for tests 3 and 5 performed with the landing gear extended. Test 7 also shows no catenary effect because of the flight path of -47.5^{o}. At this flight-path angle, the swing cables were long, and the aircraft and swing cables oscillated more slowly at about 0.25 Hz.

All aircraft crash tests performed at the facility are weather dependent. Wind velocities must be less than 4.5 m/s to insure maximum control of the aircraft in order to obtain the desired test parameters within predetermined tolerances. Winds of greater velocity acting on the aircraft can cause conditions which can result in larger errors in the aircraft attitude at impact. During test 5 a southeast wind of about 8.5 m/s velocity was experienced. The wind caused roll and yaw angle errors of approximately 3.5^{o} and displaced the aircraft 1.0 m laterally from the impact target. All other tests were made with wind velocities of less than 4.5 m/s and the aircraft experienced negligible roll and yaw errors. (See table AI.)

TABLE AI.- ANALYSIS OF ACTUAL AND PLANNED AIRCRAFT CRASH-TEST PARAMETERS

Parameter	NASA test 1		NASA test 2		NASA test 3		NASA test 4		NASA test 5		NASA test 6		NASA test 7	
	Planned	Actual	Planned	Actual	Planned	Actual	Planned	Actual	Planned	Actual	Planned	Actual	Planned	Actual
Flight-path angle, γ, deg	-15.00	-----	-15.00	-----	-18.30	-----	-15.00	-----	-18.30	-----	-15.00	-----	-45.00	-----
Flight-path angle, γ_{cs}, deg	-16.75	-16.75	-16.75	-16.00	-18.97	-18.75	-15.96	-14.75	-18.97	-20.50	-17.14	-16.50	-46.38	-47.50
Angle of attack, α, deg	.00	-----	.00	-----	.00	-----	15.00	-----	.00	-----	30.00	-----	.00	-----
Angle of attack, α_a, deg	-----	1.00	-----	4.00	-----	.75	-----	19.00	-----	1.00	-----	30.50	-----	.25
Pitch angle, θ, deg	-15.00	-----	-15.00	-----	-18.30	-----	.00	-----	-18.30	-----	15.00	-----	-45.00	-----
Pitch angle, θ_a, deg	-----	-15.75	-----	-12.00	-----	-18.00	-----	4.25	-----	-19.50	-----	14.00	-----	-47.25
Pitch angle, θ_{cs}, deg	-16.75	-16.75	-16.75	-13.50	-18.97	-18.75	-.96	3.25	-18.97	-20.00	12.86	16.50	-46.38	-47.50
Pitch angle error, θ_e, deg	.00	.00	.00	2.50	.00	.00	.00	3.00	.00	.50	.00	3.00	.00	.00
Roll angle, ϕ, deg	.00	.00	.00	.00	.00	1.25	.00	.00	.00	3.75	.00	.50	.00	.00
Yaw angle, Ψ, deg	.00	.00	.00	1.50	.00	.50	.00	-.50	.00	3.25	.00	.00	.00	2.50
Flight-path velocity, V, m/s	13.41	12.66	26.82	26.66	26.82	26.19	26.82	27.38	26.82	26.10	26.82	26.86	27.09	28.60
Vertical velocity, V_v, m/s	3.86	3.65	7.73	7.35	8.72	8.42	7.37	6.97	8.72	9.14	7.90	7.63	19.61	21.09
Horizontal velocity, V_h, m/s	12.84	12.13	25.68	25.63	25.36	24.80	25.79	26.49	25.36	24.45	25.63	25.76	18.69	19.32
Free-flight time, t, s	.15	.16	.07	.07	.07	.05	.07	.05	.07	.06	.07	.07	.07	.03
Pitching velocity, V_ω, rad/s	.20	.11	.42	.37	.17	.26	.24	.35	.17	.14	.53	.62	.34	.14
Umbilical separation time, t_u, s	1.00	No separation	1.00	1.00	.75	.78	.75	.77	.75	.77	.75	.62	.75	.74

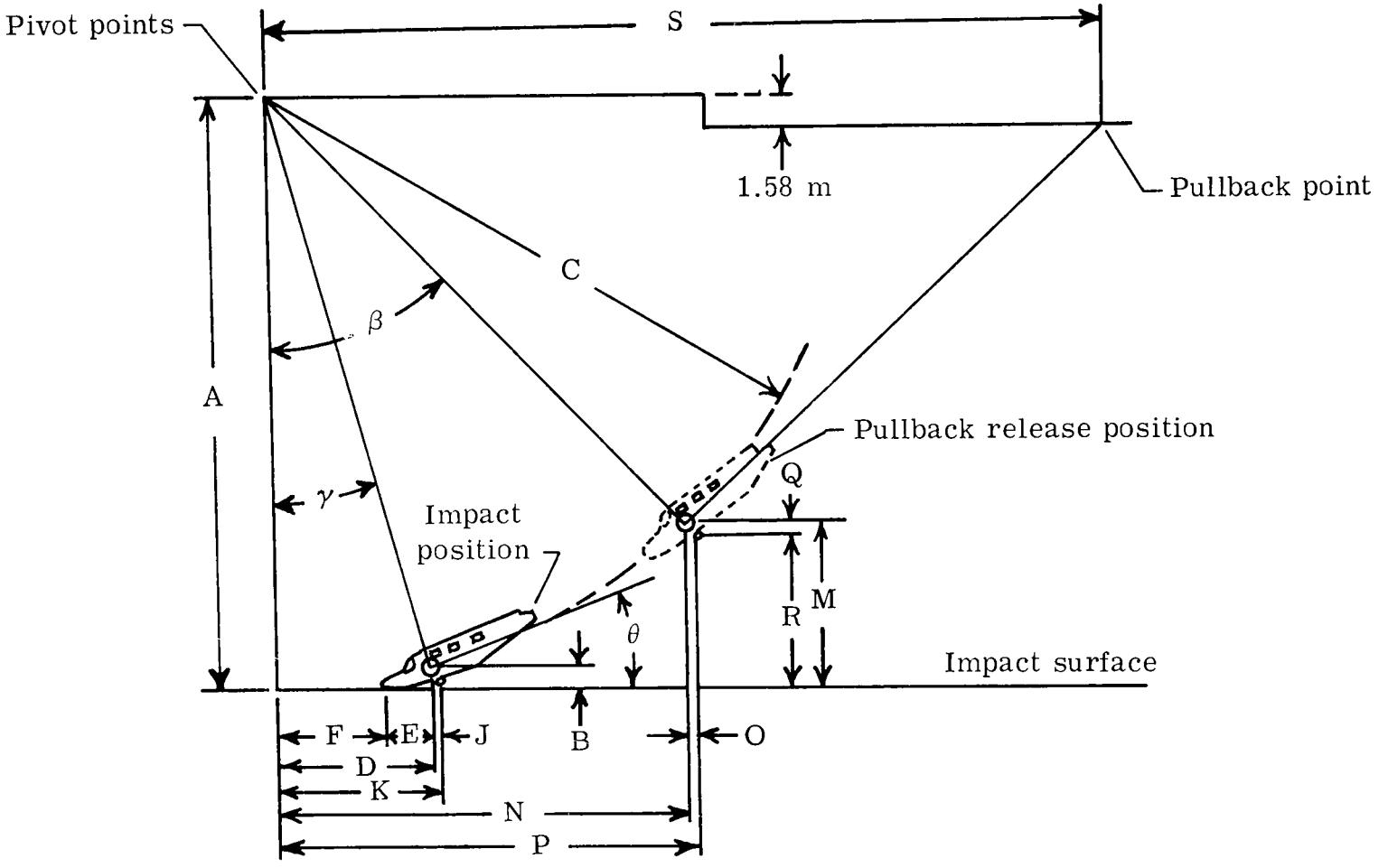

(a) Impact position and pullback release position.

Figure A1.- Aircraft crash-test geometry at impact dynamics research facility.

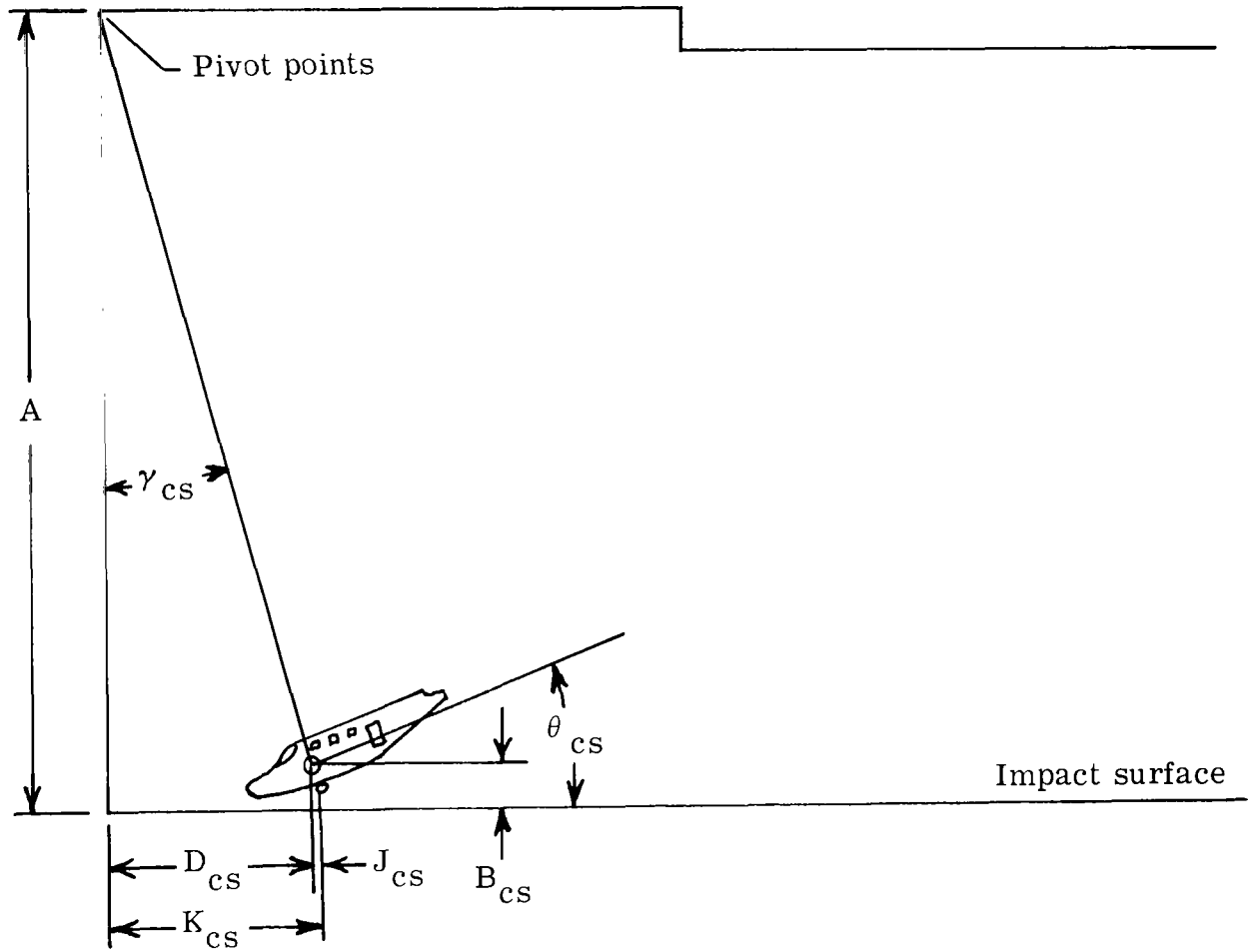

(b) Cable-separation position.

Figure A1.- Concluded.

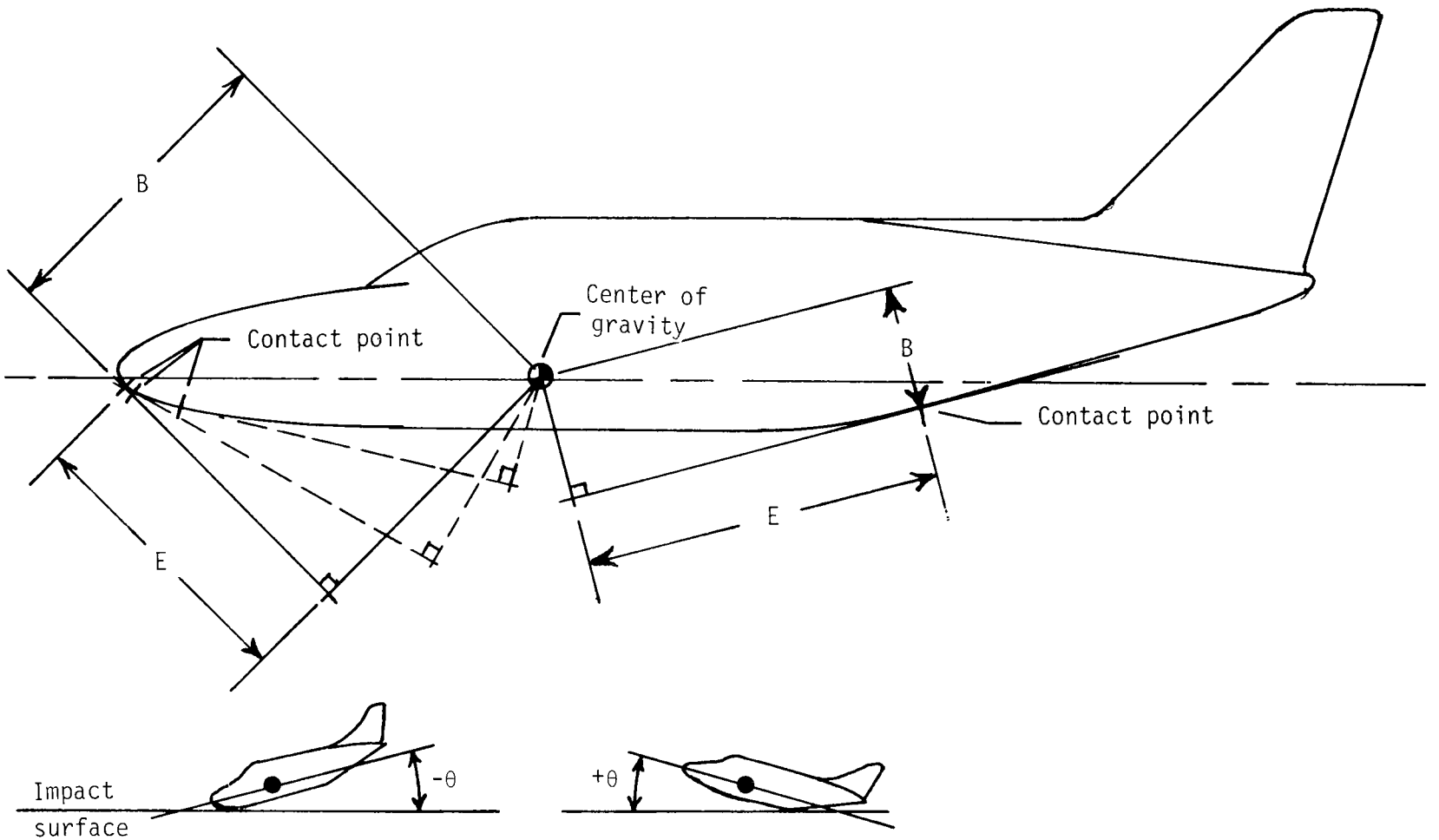

Figure A2.- Typical aircraft center-of-gravity location with respect to impact surface, pitch angle, and contact point. Dashed lines indicate various pitch angles at impact position; dimension E is negative for positive pitch angles.

APPENDIX A

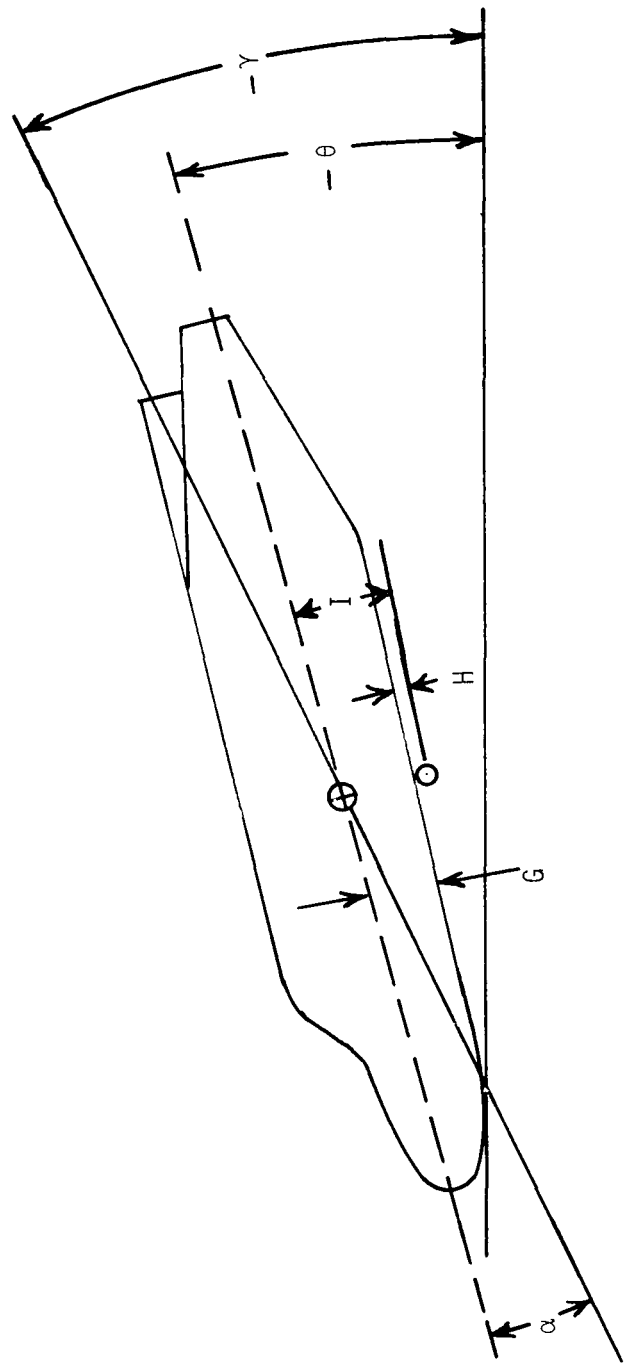

Figure A3.- Selected aircraft flight path, crash attitude, and alinement target location.

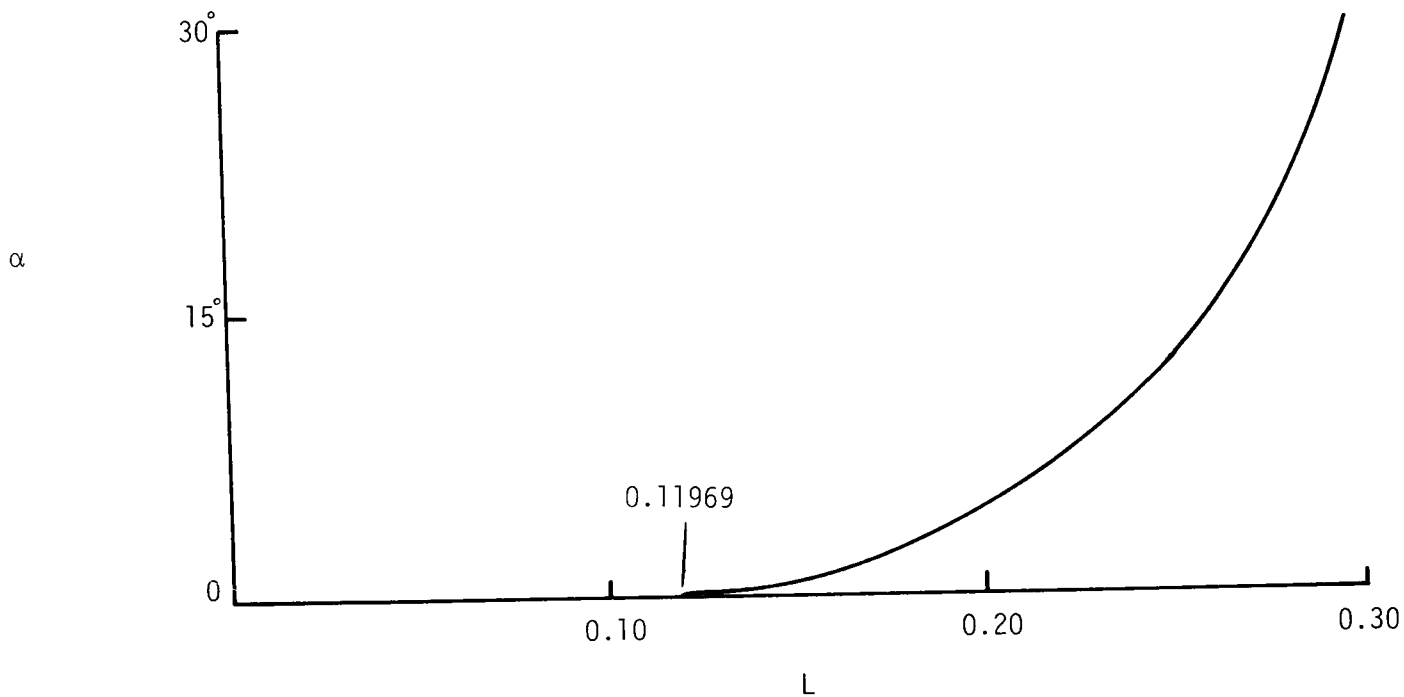

Figure A4.- Experimentally determined drag factor L for aircraft velocity of 26.82 m/s.

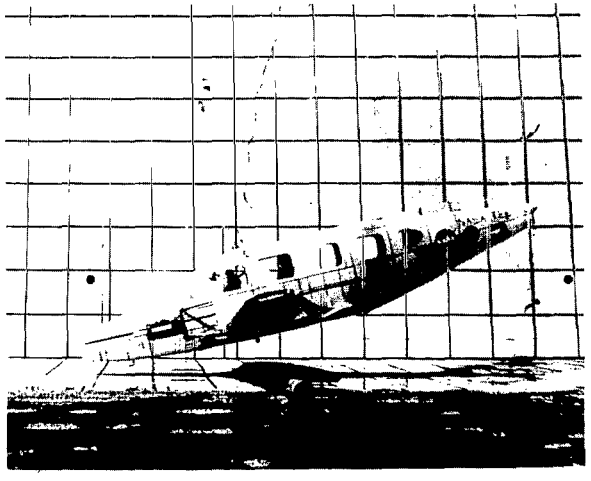

(a) Crash test 2, $\theta = -12^{o}$.

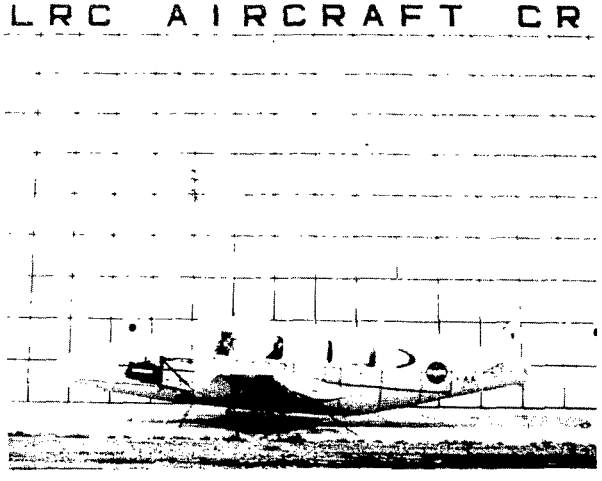

(b) Crash test 4, $\theta = 4.25^{o}$.

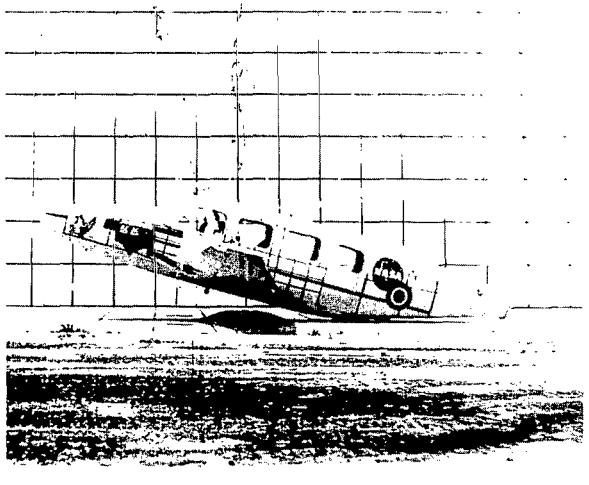

(c) Crash test 6, $\theta = 14^{o}$.

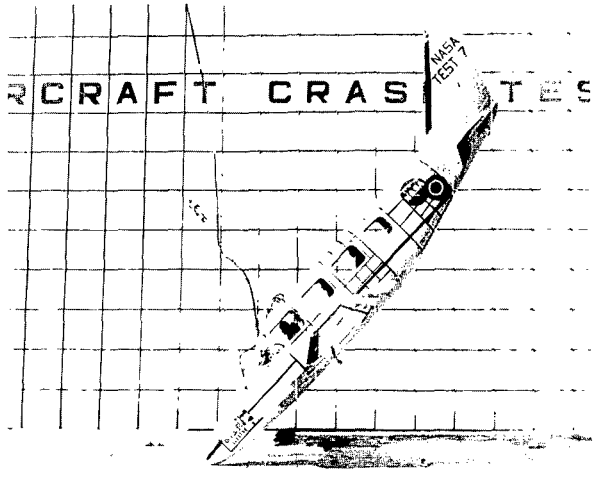

(d) Crash test 7, $\theta = -47.25^{o}$.

L-76-132

Figure A5.- Photograph showing aircraft crash attitudes for four crash tests.

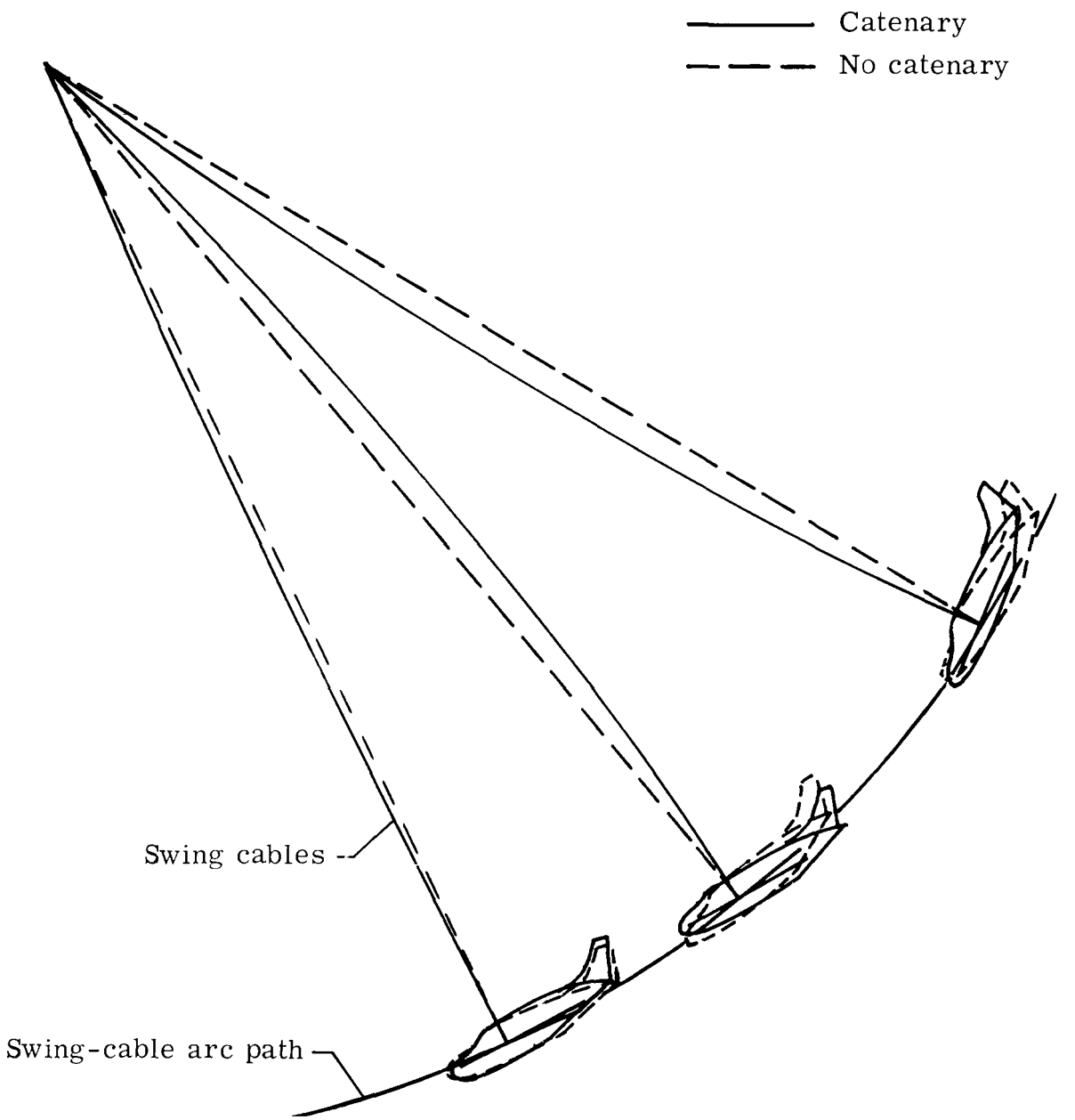

Figure A6.- Illustration of cable catenary effect on aircraft pitch angle during swing phase of test.

APPENDIX B

TEST OPERATIONS – PHASE ONE

Aircraft Crash-Test Preparation

After the aircraft is assembled with wings, empennage (or simulated mass as replacement), engines and mounts, and landing gear, the following work must be done to prepare the aircraft completely for a crash test. This work is typical and is meant only as a reference to be used as a guide to meet the requirements for the facility and test. This aircraft preparation usually takes about 6 weeks to complete. (Items are not necessarily in order.)

(1) Prepare landing gear for pneumatic operation. Drain hydraulic fluid if necessary and extend all hydraulic lines for gear and door operation outboard of port engine at trailing edge of wing.

(2) Lock all control surfaces in desired position.

(3) Paint aircraft and outline aircraft fuselage frame on exterior of fuselage. Paint on zero water line.

(4) Install swing-cable attachment hard points.

(5) Install pitch-cable attachment hard points.

(6) Install umbilical attachment plate.

(7) Install camera mounts.

(8) Install accelerometer blocks.

(9) Install mounts for instrumentation junction box, batteries, and pyrotechnic programer.

(10) Install seats and restraint systems and simulated dummies and seats if necessary.

(11) Wire interior for photographic lighting, camera controls, instrumentation, and pyrotechnic system without pyrotechnics.

(12) Install instrumentation junction box and check all wiring.

(13) Install instrumented dummies.

(14) Install cameras, batteries, pyrotechnic programer, and associated apparatus.

(15) Perform a preliminary weight and balance of aircraft.

(16) Check out pyrotechnic wiring circuits and camera circuits.

(17) Install accelerometers, connect umbilical, and check all circuits. Disconnect umbilical.